Sedimentologika

Research article

# Wet snow avalanches on Corsica Island: a long-term perspective from lake sediments

Pierre Sabatier[1], Pierre Brigode[2], Alix Bisquert[3], Nicolas Eckert[3], Florie Giacona[3], Michael Deschâtres[3], Victorien Bauve[4], Maëlle Kelner[4], Maxime Debret[5], Marie-Charlotte Bellingery[1], Yoann Copard[5], Emmanuel Malet[1], Julien Didier[6], Frédéric Huneau[4], Emilie Garel[4], Boris Vannière[7]

1 EDYTEM, Université Savoie Mont-Blanc, CNRS, 72376 Le Bourget du Lac, France
2 Université de Rennes, CNRS, Géosciences Rennes, Rennes, France
3 UMR IGE, INRAE, CNRS, IRD, Grenoble INP, Grenoble, France
4 Université de Corse, UMR CNRS 6134 SPE, Campus Grimaldi, BP52, 20250 Corte, France
5 M2C, Univ Rouen Normandie, UNICAEN, CNRS, M2C UMR 6143, F-76000 Rouen, France
6 UMR Chrono-environment, MSHE, CNRS, Université de Franche-Comté, Besançon, France
7 Institute of Plant Sciences, Oeschger Centre for Climate Change Research, University of Bern, Bern, Switzerland

*corresponding author: Pierre Sabatier (pierre.sabatier@univ-smb.fr)

doi: 10.57035/journals/sdk.2025.e31.1669

Editors: Victoria Valdez Buso and Katrina Kremer
Reviewers: Katrina Kremer and one anonymous reviwer
Copyediting, layout and production: Elizabeth Mahon, Romain Vaucher, and Francyne Bochi do Amarante

Submitted: 03.07.2024
Accepted: 04.08.2025
Published: 04.11.2025

**Abstract |** Mountain areas are very sensitive to climate change, which has led to changes in natural hazards that are often linked to disturbances in the cryosphere. In this context, changes in snowfall characteristics and snow cover affect avalanche hazards. Long-term variability can be reconstructed by using historical archives, tree rings and, more rarely, lake sediments. The latter approach is based on the identification of lake sediment consisting of poorly sorted, coarse sediments in a fine matrix, which are often associated with terrestrial organic debris. This sediment is generally brought to the lake within large amounts of wet snow, or via 'drop stones' when the ice melts if the avalanche takes place on a frozen surface. Here, we study two high-altitude lakes (Melu and Capitellu) in the Restonica Valley in Corsica, an area where systematic records are lacking, to reconstruct signals related to such large wet snow flows on a millennial scale. The analysis of several sedimentological and geochemical markers enables the characterization of wet avalanche deposits in the two lakes, as well as turbidite-type facies linked to historical earthquakes in Corsica. Age models based on short-lived radionuclides and radiocarbon also make it possible to reconstruct two avalanche chronologies covering 600 and 1750 years in Melu and Capitellu Lakes, respectively, which show similar temporal variations. A comparison with the only long-term chronology available in the Alps (Lake Muzelle, Ecrins) also reveals synchronicity in the secular variability of avalanches, suggesting a common forcing between Corsica and the Alps. Human observations and accident records from recent decades, and snow and weather release conditions reconstructed from a hydrological modeling scheme confirm the ability of the lacustrine avalanche sedimentary method to document local wet snow avalanche activity. The proposed methodology, which is based on paleolimnological studies, may therefore be useful, alone or combined with other avalanche data sources, for tracking changes in avalanche activity and related risks in mountainous areas.

**Lay summary |** Mountains are highly sensitive to climate change, which affects snowfall and the occurrence of avalanches. However, long-term records of avalanche activity are very rare, especially in regions where no systematic monitoring exists, such as the high mountains of Corsica. In this study, we use sediments preserved at the bottom of two alpine lakes to reconstruct 600 to 1,700 years of past wet-snow avalanche activity. Large avalanches reaching these lakes carry coarse debris and organic material that leave characteristic layers in the sediment. By analysing these layers and establishing precise age models, we identify when major wet-snow avalanches occurred in the past. The two lakes show similar patterns through time, and their variations match those observed in the French Alps, suggesting a common climatic influence. This work demonstrates that lake sediments provide an effective way to track avalanche activity over long periods and can help improve hazard assessment in poorly monitored mountain areas.

**Keywords**: Lake sediment; Wet avalanche; Mountain; Corisca

## 1. Introduction

Mountainous areas around the world are very sensitive to climate change, which has already altered natural hazards and related risks, especially at high elevations (IPCC, 2022; Jacquemard et al., 2024). The European mountain cryosphere notably experiences an ongoing reduction in snowfall and snow cover extent and duration (Beniston et al., 2018; Matiu et al., 2021). For example, in the French Alps, ongoing changes in snowfall and snow depth are marked (Durand et al., 2009; Verfaillie et al., 2018), and projected changes in heavy and extreme snowfall under the RCP8.5 scenario show a projected decrease below 3000 m a.s.l. and an increase above 3600 m a.s.l. (Le Roux et al., 2023). In the context of warmer temperatures, changes in snowfall and snow cover characteristics impact snow avalanche (hereafter denoted avalanches) activity (Castebrunet et al., 2014; Eckert et al., 2024). Even if precipitation remains stationary or increases moderately, a temperature increase will lead to a decrease in dry snowpack and an increase in wet snowpack (Castebrunet et al., 2014). An increase in the proportion of avalanches involving wet snow compared with avalanches involving dry snow only is therefore expected in the coming decades, associated with a shift in their timing to an earlier occurrence in the spring season in the Alps (Castebrunet et al., 2014). These projections are supported by observations or models in different mountain regions (e.g., Lazar and Williams, 2008; Naaim et al., 2016; Hao et al., 2023). We define such flows as "wet avalanches". This definition is less stringent than a definition based only on the release mechanism (e.g., Mitterer & Schweizer, 2013). In other words, our wet snow avalanches correspond both to avalanches released by wet slabs and to avalanches that incorporate wet snow during their flows, notably at lower elevations. They are typically characterized by the presence of liquid water within the deposit (Jomelli & Bertran 2001; Baggi & Schweizer, 2009).

snowpack and an increase in wet snowpack (Castebrunet et al., 2014). An increase in the proportion of avalanches in-volving wet snow compared with avalanches involving dry snow only is therefore expected in the coming decades, associated with a shift in their timing to an earlier occurrence in the spring season in the Alps (Castebrunet et al., 2014). These projections are supported by observations or models in different mountain regions (e.g., Lazar and Williams, 2008; Naaim et al., 2016; Hao et al., 2023). We define such flows as "wet avalanches". This definition is less stringent than a definition based only on the release mechanism (e.g., Mitterer & Schweizer, 2013). In other words, our wet snow avalanches correspond both to avalanches released by wet slabs and to avalanches that incorporate wet snow during their flows, notably at lower elevations. They are typically characterized by the presence of liquid water within the deposit (Jomelli & Bertran 2001; Baggi & Schweizer, 2009).

Spontaneous avalanche release and flow result from complex interactions between snowpack characteristics (depth and stratigraphy, including grain size, density and liquid water content), topography, and land cover (Schweizer et al., 2003; Mock & Birkeland, 2000; Gaume et al., 2012). Some studies have identified a clear link between avalanche occurrences and specific weather conditions, such as those in Switzerland (Laternser & Pfister, 1997) and the western United States (Mock & Birkeland, 2000). Most of these studies rely on systematic avalanche observations such as the EPA Enquête permanente sur les avalanches (Bourova et al., 2016). These are very rich in terms of documented activity (e.g., Eckert et al., 2010), but they cover only a few decades, which does not allow us to understand the centennial long-term climate impact on avalanche activity at centennial time scales. As a consequence, longer time series resulting from proxy data are needed to assess the response of natural avalanche probability and climate change, e.g., by analyzing avalanche records during the Little Ice Age (LIA) or the Medieval Climate Anomaly (MCA).

In France, as in most mountainous countries, high-elevation alpine massifs have been studied much more than lower-elevation mountain ranges (Giacona et al., 2017a). However, the latter also experiences significant avalanche activity under current climate conditions (Giacona et al., 2017b), and they may serve as sentinels to anticipate upcoming changes in snow processes and associated hazards in higher mountain environments (Giacona et al., 2021). The island of Corsica, northwest of the Mediterranean, is mostly known for its sunshine and beaches. However, with its highest peak at 2706 m a.s.l. and steep slopes with some ski resorts, it also experiences harsh winter conditions and significant avalanche activity. The Corsica mountain range is characterized by typical Mediterranean climate features with high temperatures and droughts in summer but alpine influences in winter with snow and frost (Rome & Giorgetti, 2007). The alpine belt is located above 2,000–2,100 m and is characterized by the duration of snow cover a part of the year. The deadliest avalanche in Corsican history was an avalanche that occurred at Ortiporio on 4 February 1934, which resulted in the deaths of thirty-seven people in this village (Rome & Giorgetti, 2007; Deschâtres et al., 2008). However, there is currently no systematic monitoring of avalanche activity in Corsica, and overall, avalanche risks remain poorly documented and understood across the island.

To reconstruct past avalanche activity from proxy data, many studies use dendrogeomorphology and tree-ring growth disturbances to produce a high-resolution yearly dated avalanche chronicle (Stoffel et al., 2006; Corona et al., 2010, 2013; Schläppy et al., 2013). Even if tree rings provide very valuable data, including the estimated extent of past avalanches (Favillier et al., 2018), reconstructed series are generally limited to 1-3 centuries (Eckert et al., 2024), and the capacity of trees to keep memory of past

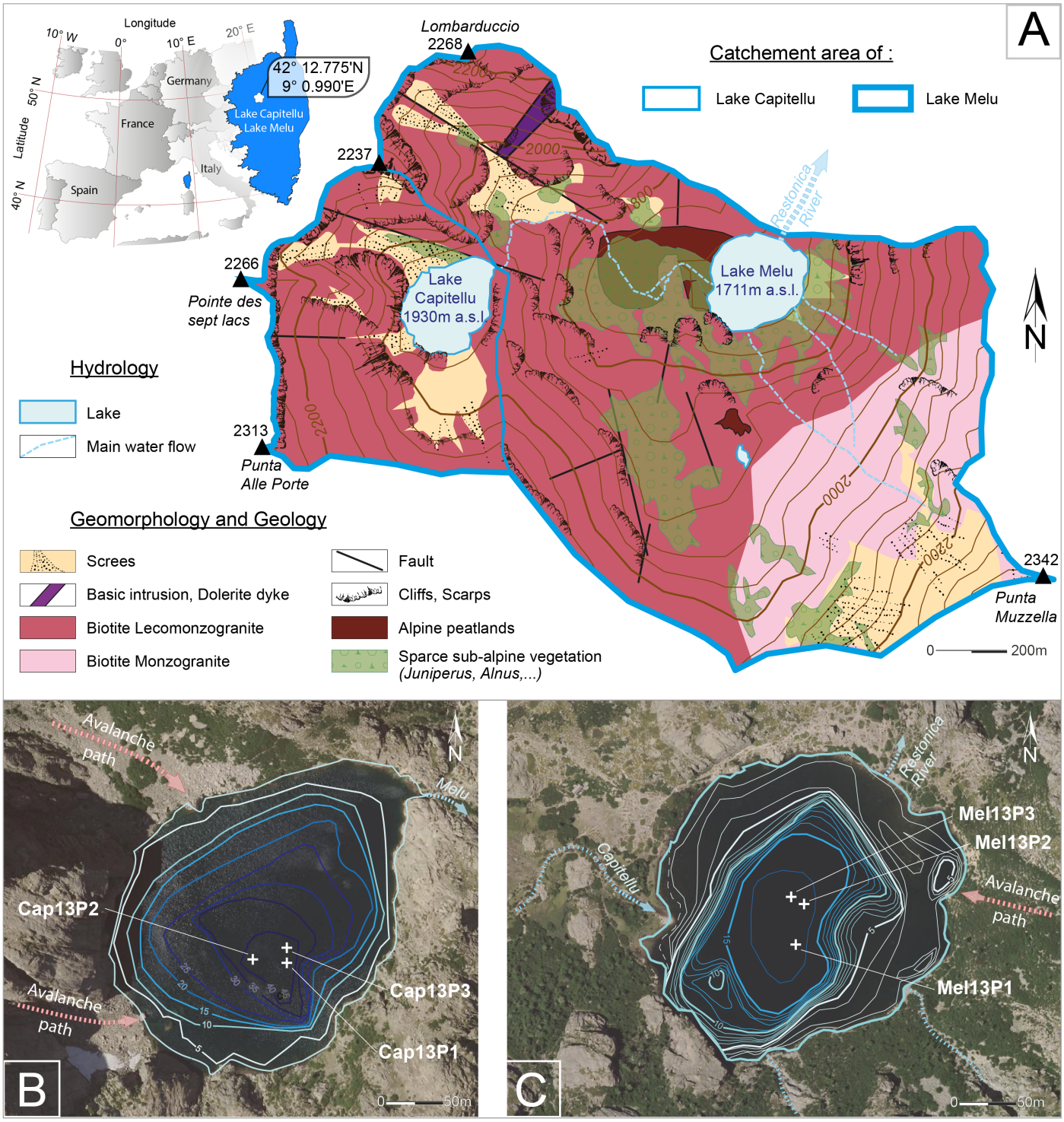


**Figure 1 |** Locations of Melu and Capitellu Lakes on Corsica Island (NW Mediterranean area). (A) Geological map with vegetation information (2020) for the two lake catchments. Aerial photographs of Lake Capitellu (B) and Lake Melu (C) with bathymetric data and the locations of the sediment cores. The red and blue dashed arrows indicate the main avalanche paths and torrent channels, respectively.

events in their rings decreases as one moves back in time (Favillier et al., 2023a). In contrast, lake sediments provide valuable archives for reconstructing avalanche deposit records over much longer periods (Sabatier et al., 2022), although with greater age uncertainties. However, this proxy has been less commonly used than, e.g., tree rings for avalanche reconstructions, and resulting local records have rarely been compared with other similar records and avalanche data from other sources. Additionally, reconstitutions from lake sediments can provide a good record only if an avalanche transports sediment that reaches the lake system, which is why only large, wet avalanches, as we define them, can be reconstructed. However, several paleolimnological studies produced wet snow avalanche chronicles in Scandinavia (Nesje et al., 2007; Seierstad et al., 2002; Vasskog et al., 2011) and, more recently, in the French Alps (Fouinat et al., 2018, 2017) and Alaska (Thys et al., 2019). Wet avalanche deposits are recorded in lake sediment as very coarse layers with very poor sorting that are sometimes associated with a fine-grained matrix and organic matter debris (Sabatier et al., 2022). When a wet avalanche occurs on a frozen lake surface, gravel can be deposited, which is subsequently identified as a dropstone in the lacustrine sediment (Thys et al., 2019).

In this study we investigate two coupled high-elevation lake systems, Lakes Melu and Capitellu in the Restonica Valley on Corsica Island (Figure 1). We reconstructed wet avalanche occurrences from lake sediment analyses via two well-dated and high-resolution multiproxy records associated with sedimentological and geochemical data. From the two resulting unusually long, wet snow avalanche chronologies, we aim to i) identify regional patterns in avalanche activity at the centennial time scale, and compare these patterns with ii) other centennial long chronologies existing in the French Alps, and iii) local records from observations and accident records from avalanches over the last century. We finally discuss the results with respect to i) the ability of lake sediments to reconstruct long centennial records of wet snow avalanche frequency, and ii) the need for improved avalanche records in Corsica and abroad.

## 2. Study sites

Lake Capitellu (5.22 ha) is a high-elevation lake (1930 m a.s.l.) with a maximum depth of 45 m that flows into Lake Melu (6.28 ha), which is set at 1711 m a.s.l. with a maximum depth of 16 m (Figure 1A). These lakes are both located in the Restonica Valley of the Monte Ritondu Massif, 10 km west of Corte city on Corsica Island (NW Mediterranean area; Figure 1A). Lake Capitellu has a restricted catchment of 48.3 ha, which is included in the Lake Melu catchment, the latter with a surface area of 227 ha and a higher point at 2342 m a.s.l. (Punta Muzzella). This catchment is mainly composed of monzogranite to leucomonanogranite which are both rich in biotite and may form coarse scree slopes, and sparse subalpine vegetation mainly around Melu Lake, and alpine peatland (Figure 1A). In the western area of the catchment, a very restricted delta is present and is composed of coarse material (coarse sand to gravel). Both lakes are frozen during a large part of the year under current climate conditions, between 6 and 7 months for Lake Melu and up to 8 months for Lake Capitellu. Different avalanche paths are present close to both lake shores (Figure 1B, C).

A set of hydrometeorological data has been aggregated at the scale of the Restonica catchment in Corte (38 km²), where a hydrometric station has been available and provides streamflow data since 2012. The SAFRAN (Système d'Analyse Fournissant des Renseignements Adaptés à la Nivologie) reanalysis data (Vidal et al., 2010) were aggregated at the scale of this catchment to produce daily time series of air temperatures and precipitation since 1959. From 1959 to 2021, the average annual temperature of this watershed was 7 °C, and the average annual precipitation was 1352 mm. The snowfall season usually begins in the Corsican Mountains at the end of October and lasts until the end of April. The maximum snow depth is generally reached between mid-February and the end of March (Rome & Giorgetti, 2007).

## 3. Materials and methods

### 3.1. Sediment coring

All sediment cores were collected in June 2013 with a UWITEC gravity corer from a small inflatable boat. Three sediment cores, referred to as CAP13P1 (IGSN (International Geo Sample Number: IEFRA006J; 34 cm), CAP13P2 (IGSN: IEFRA006K; 37 cm), and CAP13P3 (IGSN: IEFRA006L; 108 cm), were sampled at a water depth of 50 m in the central part of Capitellu Lake (42.212124° N, 9.012468° E) (Figure 1B). Three sediment cores, referred to as MEL13P1 (IGSN: IEFRA009X; 50 cm), MEL13P2 (IGSN: IEFRA009Y; 25 cm), and MEL13P3 (IGSN: IEFRA009Z; 137 cm), were sampled in the central part of Melo Lake (42.213017° N, 9.022909° E) at a water depth of 16 m (Figure 1C). All the core metadata are stored in the French Cyber-Core repository (https://cybercarotheque.fr/).

### 3.2. Sedimentological analyses

At the EDYTEM laboratory, cores were split, photographed, and logged in detail, and all physical sedimentary structures and the vertical succession of facies were noted for further correlation.

For the very coarse sedimentary material, grain size was determined on cores CAP13P3 and MEL13P3 by wet sieving sediment samples from different meshes (5 mm, 3.15 mm, 2 mm, 1.25 mm and 1 mm); then, dry sediment weight was measured for each fraction. A fraction smaller than 1 mm was measured through a laser granulometer using a Malvern Mastersizer 2000G with ultrasound to minimize particle flocculation. Based on the weight estimations, a complete grain size distribution between 10 mm and 0.02 µm was subsequently calculated, and different grain size parameters were calculated with GRADISTAT (Blott and Pye, 2001). Additionally, a gravel–sand–mud ternary diagram was produced via QGrain (Liu et al., 2021). Samples for grain size analyses were taken from identified event deposits larger than 5 mm in the two cores, with the resolution adapted accordingly.

Samples for dry bulk density (DBD) and loss on ignition (LOI) were taken at a 1 cm resolution, adapted to sedimentary boundaries within the identified background sedimentation (few on event deposits) in CAP13P3 (n = 53) and MEL13P3 (n = 51). The organic matter content was estimated through LOI550 following the protocol of Heiri et al. (2001), and these cores had no carbonate content.

### 3.3. Geochemical analyses

X-ray fluorescence (XRF) analyses were performed on the surfaces of the split sediment cores at 1 mm intervals via a non-destructive Avaatech core scanner (EDYTEM lab). The geochemical relative components (intensities), expressed in counts per second, were obtained at various

tube settings: 10 kV at 1.5 mA for 40 s for Al, Si, S, K, Ca, Ti, Mn, and Fe and 30 kV at 1.2 mA for 60 s for Cu, Zn, Br, Sr, Rb, Zr, and Pb. The single-element relative abundances are expressed as centred log ratios (CLRs) to avoid matrix effects inherent to these data types (Weltje et al., 2015). All the measured elements were taken for the geometric mean calculation needed for the CLR, except for Mn, because it has a low intensity and a noisy signal. Principal component analysis (PCA) was performed on the non-transformed XRF data of the MEL13-P3 and CAP13-P3 cores to determine the geochemical endmembers (Sabatier et al., 2010).

A continuous sampling step, adapted to sedimentary boundaries of 5 mm, was applied over the first 10 cm of CAP13P1 (n = 16), and a step of 1 cm was applied to the first 25 cm of MEL13P2 (n = 25) to determine $^{210}$Pb, $^{226}$Ra, $^{137}$Cs and $^{241}$Am activities via well-type germanium detectors placed at the Laboratoire Souterrain de Modane following Reyss et al. (1995). For each sample, the $^{210}$Pb excess activity was calculated by subtracting the $^{226}$Ra-supported activity from the total $^{210}$Pb activity measured. The sediment core chronology was then carried out over the last 120 years via the R package "serac" (Bruel and Sabatier, 2020) and the constant flux constant sedimentation (CFCS) model, which was validated with artificial radionuclides ($^{137}$Cs and $^{241}$Am).

Eight radiocarbon analyses of organic plant macroremains, 4 on the CAP13P3 core and 4 on the MEL13P3 core, were performed via accelerator mass spectrometry (AMS) at the Poznan Radiocarbon Laboratory. The $^{14}$C ages were calibrated via the Intcal20 calibration curve (Reimer et al., 2020). The two lake age models were calculated via the R code package clam (Blaauw, 2010).

### 3.4. Human observations of avalanche activity in the area

To evaluate and discuss the reconstruction of avalanche activity from sediment records, we compiled different sources related to human observations of avalanches in the area. Given that the studied lakes are situated in a remote zone, we extended the search to the entire upper Restonica Valley down to the lake catchments (Figure 1). Sources include accident records collected at the national scale by the ANENA (Techel et al., 2016), testimonies and observations by local technicians from meteorological and state services, a participatory web-based database about snow avalanches (https://www.data-avalanche.org/) and the EPA. Notably, the latter was active in Corsica only between c. 1970 and 1985.

### 3.5. Hydrometeorological modeling over the last 6 decades

To better understand the meteorological conditions leading to avalanches in this region, the historical hydrometeorological conditions of the Restonica catchment in Corte (38 km²), especially the upper part where the two studied lakes are located, have been reconstructed through hydrological modeling over the past six decades. For this purpose, the GR4J rainfall-runoff model (Perrin et al., 2003) and its snow accumulation and melt module CemaNeige (Valéry et al., 2014) were calibrated with the available data.

GR4J is a reservoir-based model characterized by four parameters that need to be calibrated for each catchment, which allows for the simulation of daily streamflow series from daily precipitation and potential evapotranspiration series. Precipitation data were extracted from the SAFRAN reanalysis (Vidal et al., 2010), and potential evapotranspiration data were also estimated via air temperature series from the SAFRAN reanalysis and the formula from Oudin et al. (2005), which was developed for this specific objective of hydrological modeling.

The CemaNeige module simulates snow accumulation and melting over time on the basis of two parameters to be calibrated: a series of catchment air temperatures and an elevation distribution of the watershed. From this elevation distribution, the catchment is divided into elevation bands (5 in this case), for which meteorological conditions are interpolated/extrapolated from the general catchment meteorological conditions. Thus, for each elevation band, a daily snowpack is simulated according to the meteorological conditions. The evolution of these different snowpacks is then combined at each modeling timestep to achieve a comprehensive hydrological balance of the watershed and thus simulate streamflows.

The calibration of the GR4J model parameters and its CemaNeige snow module was carried out simultaneously over the period 2009–2022 (the period of availability of the streamflow data), using the R package airGR (Coron et al., 2017; 2022) and the Kling-Gupta efficiency criterion (Gupta et al., 2009) as the objective functions.

Once the parameters were calibrated and the consistency of the model performance was confirmed, the six parameters were used to simulate the temporal evolution of the snowpack and streamflows over the entire SAFRAN period from 1959–2022. This reconstruction allows for the analysis of the hydrometeorological conditions associated with avalanche observations over the recent period. This type of hydrometeorological reconstruction has already been used in the context of comparisons with sedimentary proxies in different settings (e.g., Brigode et al., 2016; Gagnon-Poiré et al., 2021).

## 4. Results

### 4.1. Sedimentary description

The sediments from both the MEL and CAP cores consist mainly of dark green organic-rich silt facies (F1) corresponding to lake background sedimentation (Figure 2A,

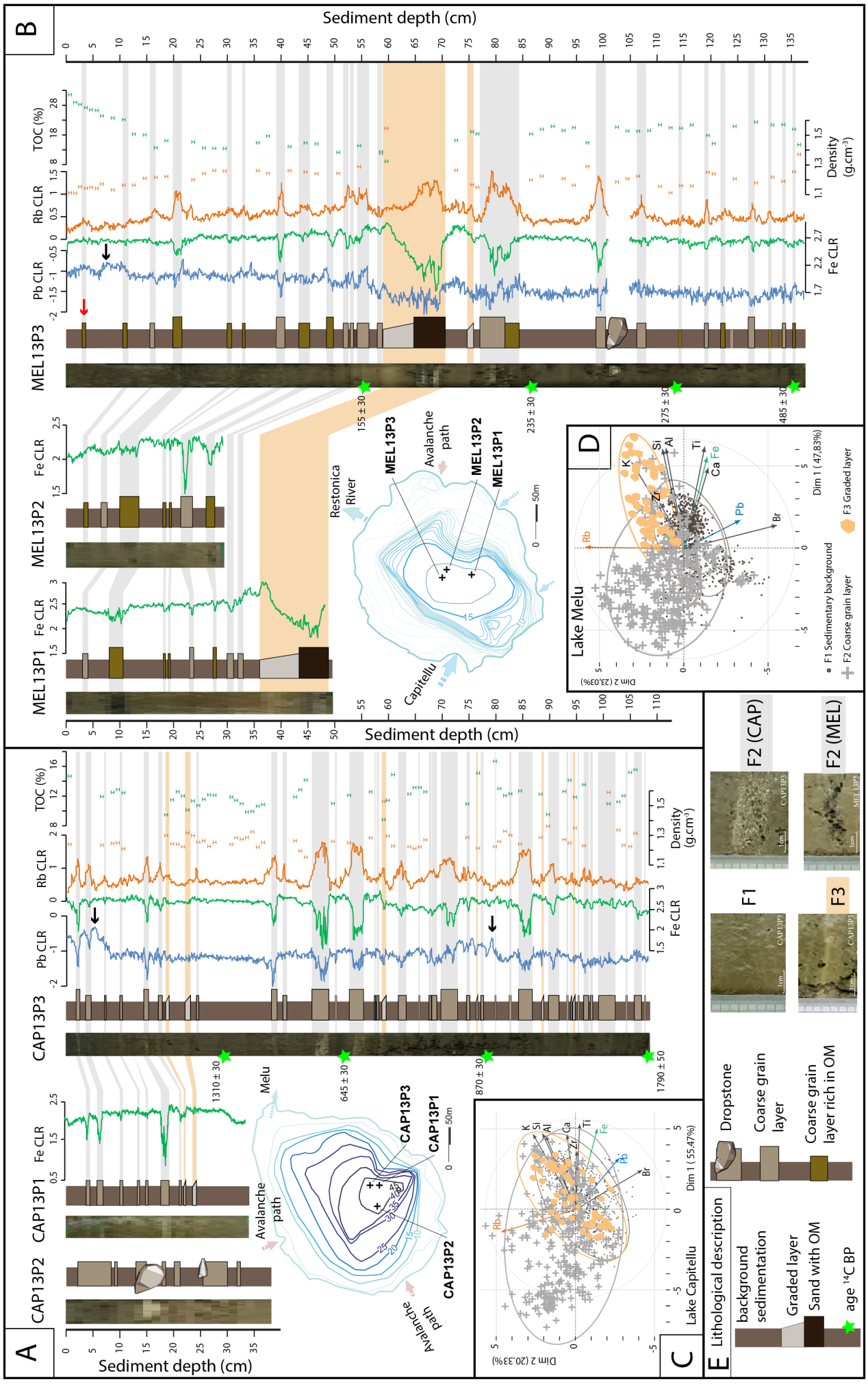


**Figure 2 |** Pictures, sedimentary descriptions and selected element contents in cores CAP13P1, CAP13P2, and CAP13P3 in A and MEL13P1, MEL13P2, and MEL13P3 in B. Gray and orange bands indicate thicker than 5 mm F2 and F3 event deposit correlations, respectively. Biplots from PCA of geochemical content are illustrated in C and D for CAP13P3 and MEL13P3, respectively. Lithological description is indicated in E. The PCA depths are illustrated with respect to sedimentary descriptions (F1 in dark gray, F2 in gray and F3 in orange). Black arrows indicate Pb peaks, and red arrows indicate the March 2005 wet avalanche deposit, as illustrated later in Figure 6B.

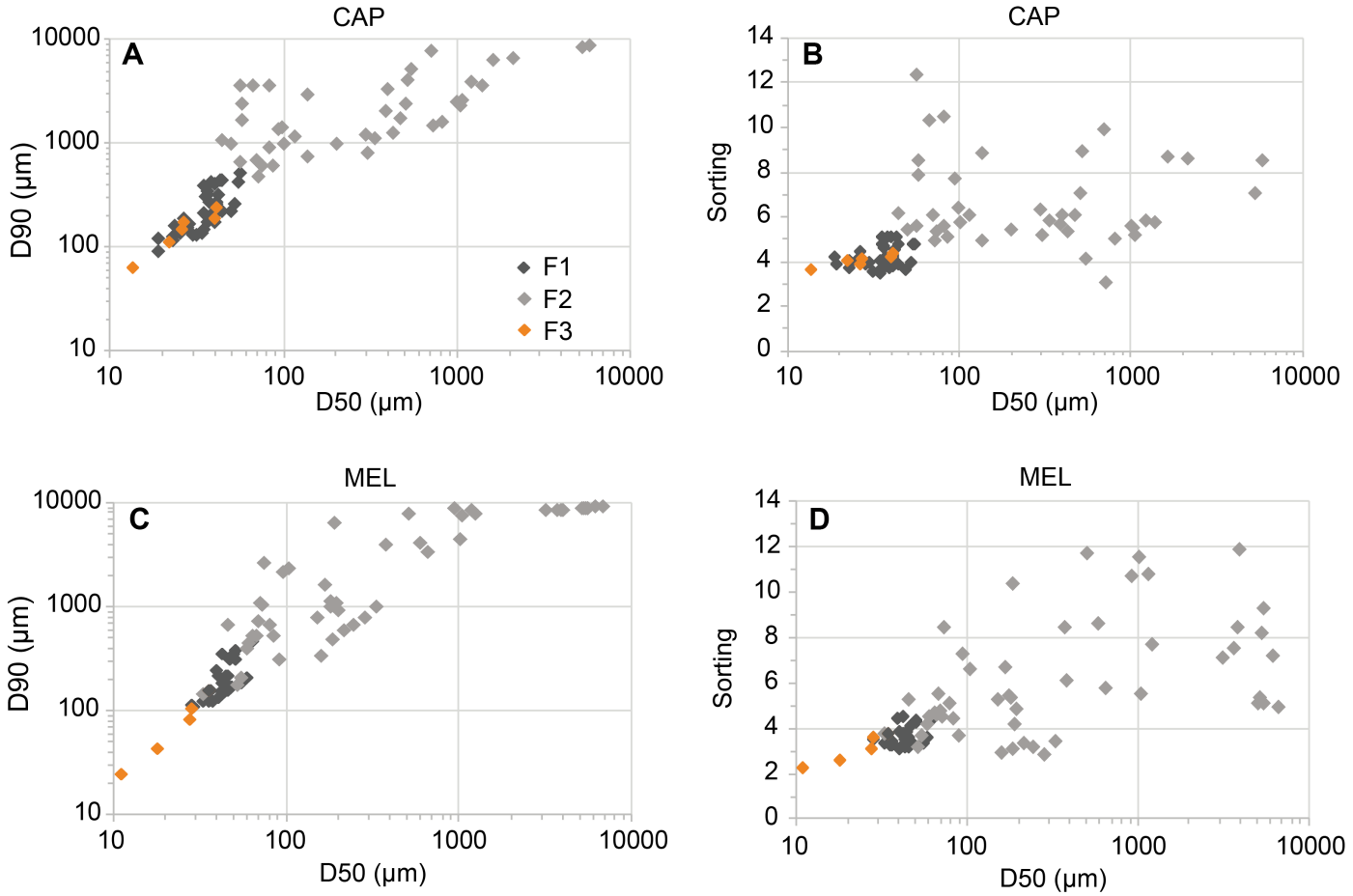


**Figure 3 |** Grain size data for CAP13P3 (A and B) and MEL13P3 (C and D) according to facies descriptions (F1: dark gray, F2: gray and F3: orange). Biplots of D50 versus D90 and D50 versus Sorting are shown.

B). This facies presents relatively high organic matter content, with mean LOI550 values of 19.4 ± 4.7 % and 12.5 ± 1.4 % for MEL and CAP, respectively (Figure 2A, B). In this facies, the dry bulk density (DBD) exhibited little variation, with mean values of 1.20 ± 0.06 and 1.30 ± 0.10 g.cm$^{-3}$ for MEL and CAP, respectively (Figure 2A, B). The carbonate is not detectable through LOI950. The grain size data indicate poorly to very poorly sorted (Sorting = 3.6 MEL/4.3 CAP) silt with a mean grain size of D50 = 43 ±9 µm for MEL and D50 = 38 ±10 µm for CAP (Figure 3). This homogeneous background sedimentation is interrupted by two types of event deposits, namely, facies 2 (F2) and facies 3 (F3) (Figure 2A, B).

F2 corresponds to a mixture of gravel, mud, and sand (Figure 2A, B and S1) in both cores, and is associated with organic matter debris in the MEL cores (Figure 2B). Some of these gravel layers are normal grading. The DBD in F2 was slightly greater than that in background sedimentation, with average values of 1.21 ± 0.05 and 1.33 ± 0.03 g.cm$^{-3}$ for MEL and CAP, respectively, and the LOI550 values were 19.7 ± 3.3 % and 10.4 ± 1.0 % for MEL and CAP, respectively, with a significantly lower content for CAP (Figure 2A, B). We identify 29 F2 deposits ranging from 4–47 mm thick in MEL13P3, and 32 F2 deposits ranging from 3–60 mm thick in CAP13P3. The grain size data indicate very poorly sorted (sorting = 6.2 MEL/6.8 CAP) sediment with a mean grain size of D50 = 1280 ±2000 µm for MEL and D50 = 688 ±1200 µm for CAP (Figure 3).

F3 corresponds to graded green silt with a light clay cap at the top (Figure 2A, B and S1) in both cores. In the MEL cores, the base of one of these deposits is composed of sand with a high amount of organic matter debris (70 cm in MEL13P3, Figure 2B). The DBD in F3 was greater than that in background sedimentation and F2, with values of 1.46 ± 0.12 and 1.53 g.cm$^{-3}$ (one value) for MEL and CAP, respectively, and the LOI550 was lower in F3, with values of 10.7 ± 2.2 % and 8.9 % (one value) for MEL and CAP, respectively (Figure 2A, B). We identify 2 F3 deposits ranging from 9–115 mm thick in MEL13P3 and 7 F3 deposits ranging from 4–25 mm thick in CAP13P3. The grain-size data indicate poorly sorted (Sorting=3.2, MEL/4 CAP) silt with a mean grain size of D50 = 35 ± 11 µm for MEL and D50 = 28 ± 11 µm for CAP (Figure 3).

The grain size data according to the facies descriptions are shown in Figure 3 for CAP13P3 and MEL13P3. F1 presented a relatively well-constrained group of values in both cores. F2 displays a large range of variability, with coarse and very poorly sorted sediment without a grain size trend. F3 contains finer sediments with better sorting and shows a linear relationship between D50 and D90 in both cores, which partly overlap with the F1 group, especially in the CAP13P3 core (Figure 3A).

### 4.2. Geochemistry

PCA of the selected raw XRF data is shown in Figure 2C and D. Biplots of the first 2 dimensions (Dim1 and Dim2) on MEL13P3 and CAP13P3 present 76 and 71 %, respectively, of the total variability. The two PCAs have similar structures and allow the identification of 3 geochemical endmembers: 1) high positive loadings of K, Al, Si, Ti, Ca, Fe and Zr on Dim1; 2) high positive loadings of Rb on Dim2; and 3) negative loadings of Pb and Br on Dim2. The addition of sedimentary facies allows the distribution of geochemical data to be mapped via PCA (Figure 2C, D). Mapping revealed that F1 and F3 had similar distributions with relatively high Dim1 values at MEL and small differences in CAP, with lower Dim2 values at F3 than at F1. A portion of F2 overlaps F1 and F3, but a large part of the data shows negative values for Dim1 and positive values for Dim2 in both cores.

The downcore variations in one element (Fe, Pb, Rb) for each geochemical endmember are shown in Figure 2A and B. F1 and F2 present anticorrelated variations, with high Fe contents and low Rb contents in F1, whereas F2 shows high Rb and low Fe contents. F3 has a different pattern of element variation within the facies, with relatively high Rb content at the base, and an increase in Fe content toward the upper part of the facies, with higher Fe values occurring in the light clay cap at the top. In MEL13P3 the Pb content varies little, with higher Pb content in organic-rich F2 deposits, and relatively lower Pb content in gravel- and sand-dominated F2 deposits (Figure 2B). We also observed higher Pb content in the upper 12 cm (F1) of the core. In CAP13P3, the Pb content was relatively low in F2 and F3, and there were long-term variations in F1, with higher Pb content occurring within the first 8 cm and between 73 and 82 cm (Figure 2A).

### 4.3. Core correlation

On the basis of lithological descriptions and XRF downcore variations it is possible to correlate cores from the same lake (Figure 2A, B). In Capitellu Lake, F2 and F3 in

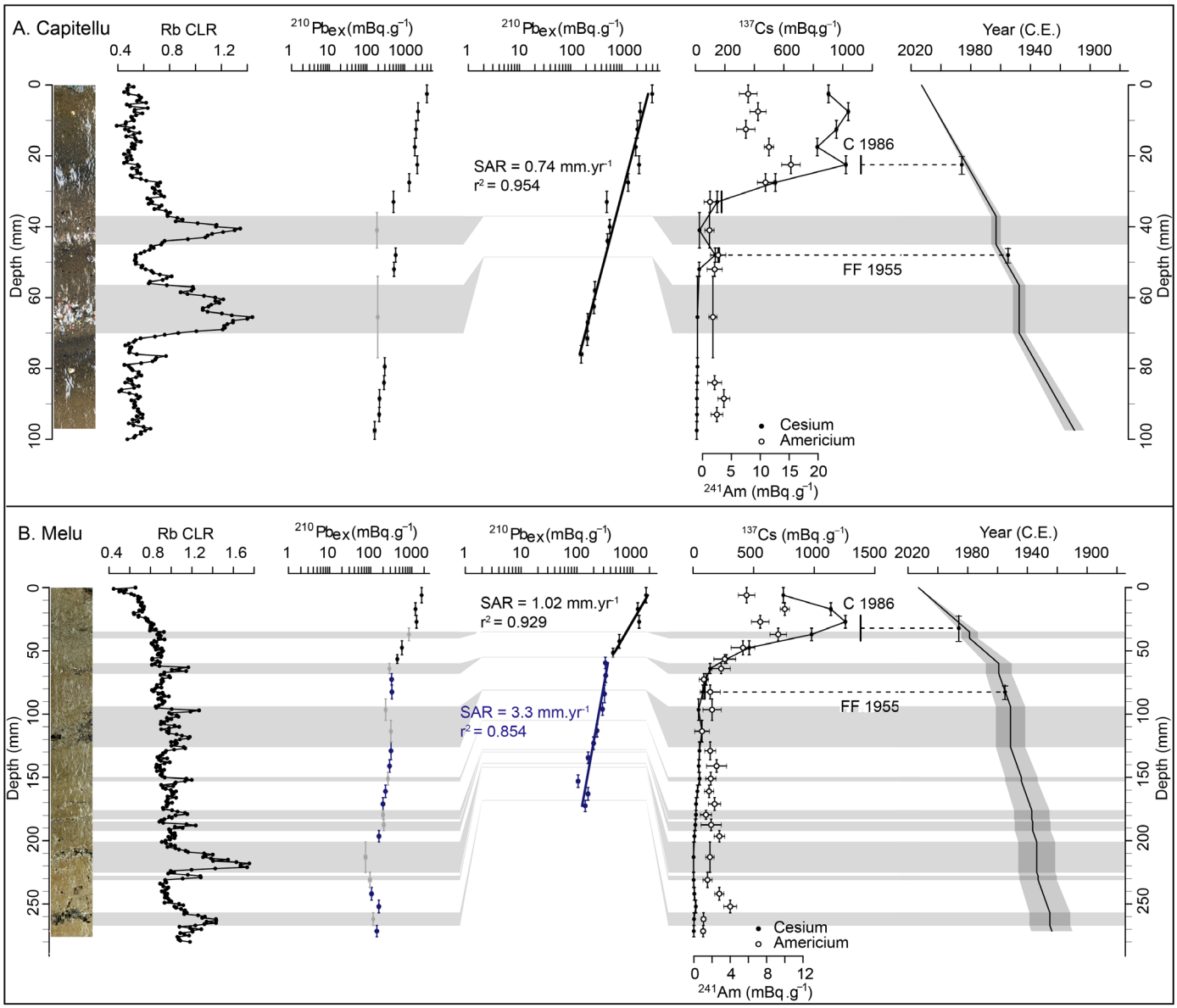


**Figure 4 |** Chronology based on short-lived radionuclides for the CAP13P1 (A) and MEL13P2 (B) cores. From left to right: picture, Rb CLR, $^{210}$Pbex activities, event deposit-corrected $^{210}$Pbex activities, $^{137}$Cs and $^{241}$Am activities, and the CFCS age model. The event deposits are highlighted by horizontal gray bands. FF: first fallout in 1955, C: Chernobyl accident 1986.

the CAP13P1 and CAP13P3 cores can be easily correlated, with thick F2 deposits showing a decrease in thickness from P1 to P3, toward the northeast (Figure 2A). CAP13P2 contains very coarse materials with rock pieces of several centimeters in diameter, which excludes both XRF-based and visual correlations with P1 and P3, but these very coarse rock fragments indicate that the material origin for F2 was probably the southeastern part of the catchment, where we also observed an avalanche corridor (Figure 1B). In Melu Lake, F2 and F3 were well correlated within all 3 cores. Owing to the short lengths of cores CAP13P1 and P2, only the 2 upper F3 deposits in CAP13P3 are correlated with the other 2 cores (orange bands in Figure 2A), which have approximately the same thickness and grain size. For F2 deposits, fewer events with less coarser materials are present at MEL13P1 (southern position), and thicker events are present at MEL13P2 and MEL13P3 (Figure 2B). The correlations between these two cores indicate a relatively small decrease in thickness toward the west, which could indicate the input of coarse material from the east corresponding to the corridor avalanche (Figure 1C).

### 4.4. Chronology

The chronological framework was based on short-lived radionuclides for sediment from the last century, and on radiocarbon ages for intervals older than the last century for the two cores.

Short-lived radionuclides were treated with the R package serac (Bruel and Sabatier, 2020). In the CAP13P1 and MEL13P2 cores, the F2 deposits are enriched in the Rb CLR, leading to the identification of 2 and 8 event deposits respectively (gray bands in Figure 4A, B), no F3 deposits are identified in these upper core parts. These F2 events were considered instantaneous and thus excluded from the age model construction by removing the depth interval and associated $^{210}$Pbex data of each of these intervals (Bruel and Sabatier, 2020). The logarithmic plot of the event-corrected $^{210}$Pbex activity shows a well-constrained decrease in the CAP13P1 core, which allows us to calculate the mean sedimentation rate from the "constant flux, constant sedimentation rate" (CFCS) at 0.74 ± 0.05 mm.y$^{-1}$ (Figure 4A). Ages were then calculated via the CFCS model applied to the original sediment sequence (with event deposits) to provide a continuous age–depth relationship. The $^{137}$Cs profile presented one peak between 20 and 25 mm, with a very high activity of 1021 ± 7 mBq.g$^{-1}$, which probably corresponded to the Chernobyl accident in 1986 CE. At this depth, we also observed an increase in 241Am activity in relation to high $^{137}$Cs Chernobyl fallout, as already observed in Italy (Rapuc et al., 2019). The first $^{137}$Cs increase was observed between 50 and 54 mm and could correspond to 1955 CE and the first $^{137}$Cs global fallout (Figure 4A). The maximum nuclear fallout in 1963 CE in the Northern Hemisphere was probably hidden by 1) the very important Chernobyl peak, 2) the relatively low sedimentation rate and 3) the low sampling resolution. This age model is confirmed by the good agreement between the $^{210}$Pbex and $^{137}$Cs markers. The logarithmic plot of the event-corrected $^{210}$Pbex activity shows two well-constrained distinct linear trends in MEL13P2, which allows us to calculate 2 mean sedimentation rates from the CFCS model: 1.02 ± 0.16 mm.y$^{-1}$ from 0–60 mm and 3.30 ± 0.48 mm.y$^{-1}$ from 60–270 mm (Figure 4B), with a change occurring at 1961 ± 6 years. For the CAP13P1 core, the $^{137}$Cs profile at MEL13P2 presented one peak between 22 and 32 mm, with a very high activity of 1257 ± 6 mBq.g$^{-1}$, associated with high $^{241}$Am activity, which probably corresponded to the Chernobyl accident in 1986 CE (Figure 4B). The first $^{137}$Cs increase is not easy to identify because $^{137}$Cs activity is still detectable at the base of the core, probably because of the high water availability, which could migrate in the sediment and along the liner after core collection. Both age models provide an age for these upper event deposits.

Four terrestrial organic macroremain samples were dated by $^{14}$C age from both the CAP13P3 and MEL13P3 cores (Table 1) and calibrated via the Intcal20 calibration curve (Reimer et al., 2020). One radiocarbon age in the CAP13P3 core was excluded because it appeared to be too old, probably because macroremains were stored in the lake catchment before being transported in the lake (Figure 5A). The cumulative F2 and F3 event deposits interpreted as instantaneous deposits (Figure 2), are 35.1 cm and 38.1 cm long for CAP13P3 and MEL13P3 respectively, and were removed before age modeling. The remaining sediment sections of the two lakes were used to construct two event-free sedimentary records (Sabatier et al., 2022). We then calculated the age-depth

| Samples | Material dated | Cores | Depth (mm) | Uncalibrated age (BP) | Uncertainty | Calibrated age ranges at 95% confidence interval (cal. BP) |
|---|---|---|---|---|---|---|
| Poz-96970 | O. Macro | CAP13P3 | 290 | 1310 | 30 | 1182–1293 |
| Poz-96972 | O. Macro | CAP13P3 | 515 | 645 | 30 | 556–668 |
| Poz-96971 | O. Macro | CAP13P3 | 785 | 870 | 30 | 704–904 |
| Poz-61155 | O. Macro | CAP13P3 | 1095 | 1790 | 50 | 1570–1857 |
| Poz-96983 | O. Macro | MEL13P3 | 555 | 155 | 30 | 0–284 |
| Poz-96984 | O. Macro | MEL13P3 | 865 | 235 | 30 | 0–421 |
| Poz-96969 | O. Macro | MEL13P3 | 1135 | 275 | 30 | 153–450 |
| Poz-61156 | O. Macro | MEL13P3 | 1355 | 485 | 30 | 501–543 |

**Table 1 |** Radiocarbon ages uncalibrated and calibrated for the CAP13P3 and MEL13P3 cores. The age highlighted in bold is not considered for age modeling.

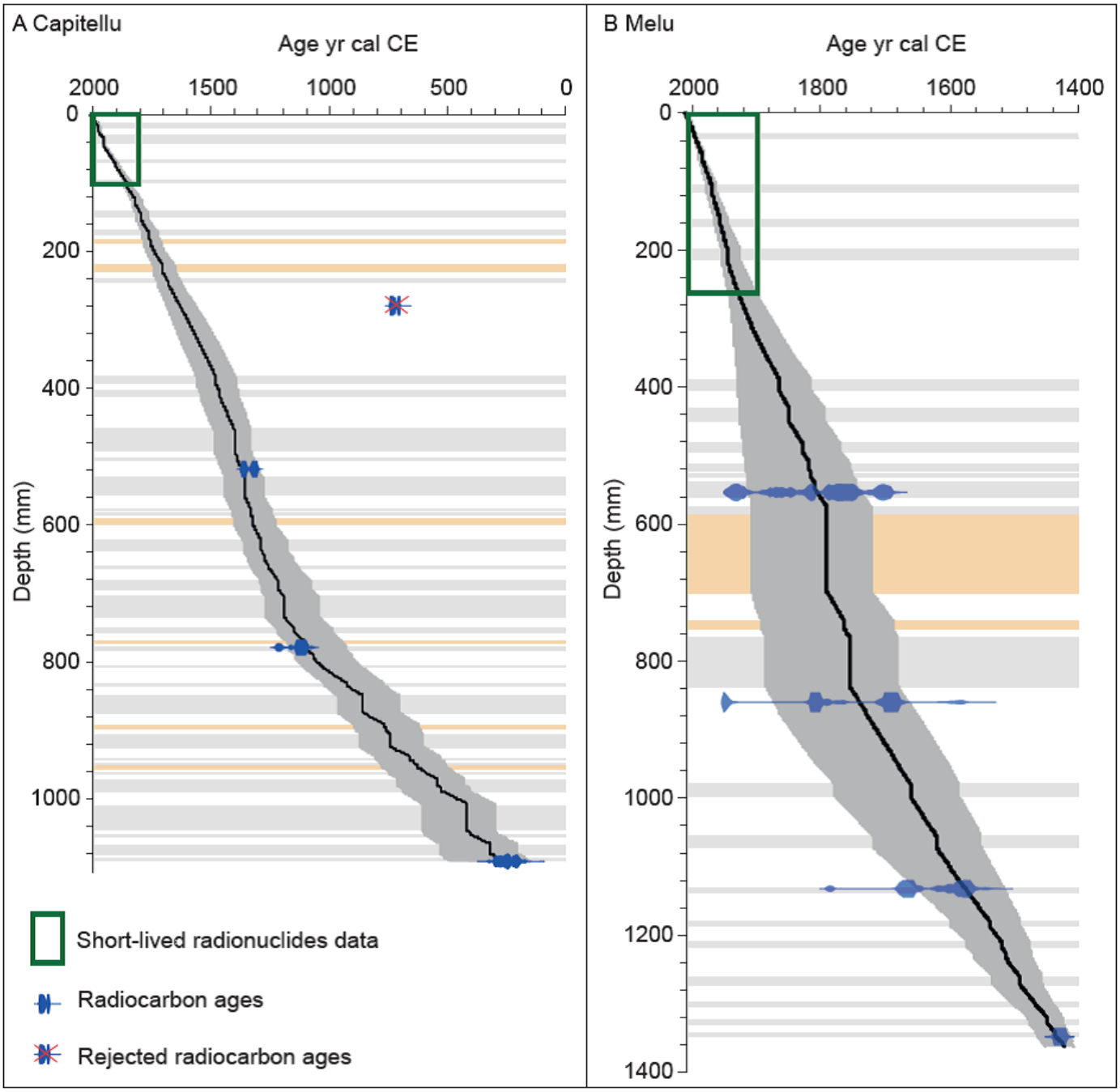


**Figure 5 |** Age models for the CAP13P3 (A) and MEL13P3 (B) cores based on short-lived radionuclides (green rectangle) and $^{14}C$ ages (blue age distribution). The gray and orange bands indicate thicker F2 and F3 event deposits, respectively.

relationship for each lake via smooth spline interpolation via the R package Clam (Blaauw, 2010) on the basis of $^{14}C$ ages and correlated short-lived radionuclide ages, which allowed us to date all event deposits, represented by the vertical bars in Figure 5. The first 108 cm of CAP13P3 for and 137 cm of MEL13P3 covered the last 1750 and 580 years, respectively.

### 4.5. Avalanche chronology from human observations in the upper Restonica

The different sources of human observations allowed the retrieval of 20 avalanches in the upper Restonica: 13 from the EPA, 3 from the ANENA (accident reports), 3 from testimonies and observations by local technicians, and one from the participatory database data-avalanche.org.

These events are related to 6 distinct avalanche paths, with 5 to 1 single avalanches per path. Four avalanches could not be localized at the path scale but occurred within the upper Restonica with certainty (Figure 6A). All the avalanches that could be localized at the path scale occurred in paths that were part of the active EPA in Corsica, except for one avalanche that reached Melu Lake in early March 2005 (Figure 6B). This March 2005 avalanche was the only avalanche for which wet snow was reported to be involved and that reached Melu Lake; for all other avalanches, the nature of the snow involved was not explicitly documented. Note that two other paths from the valley were also part of the EPA but that no avalanche was recorded in these paths.

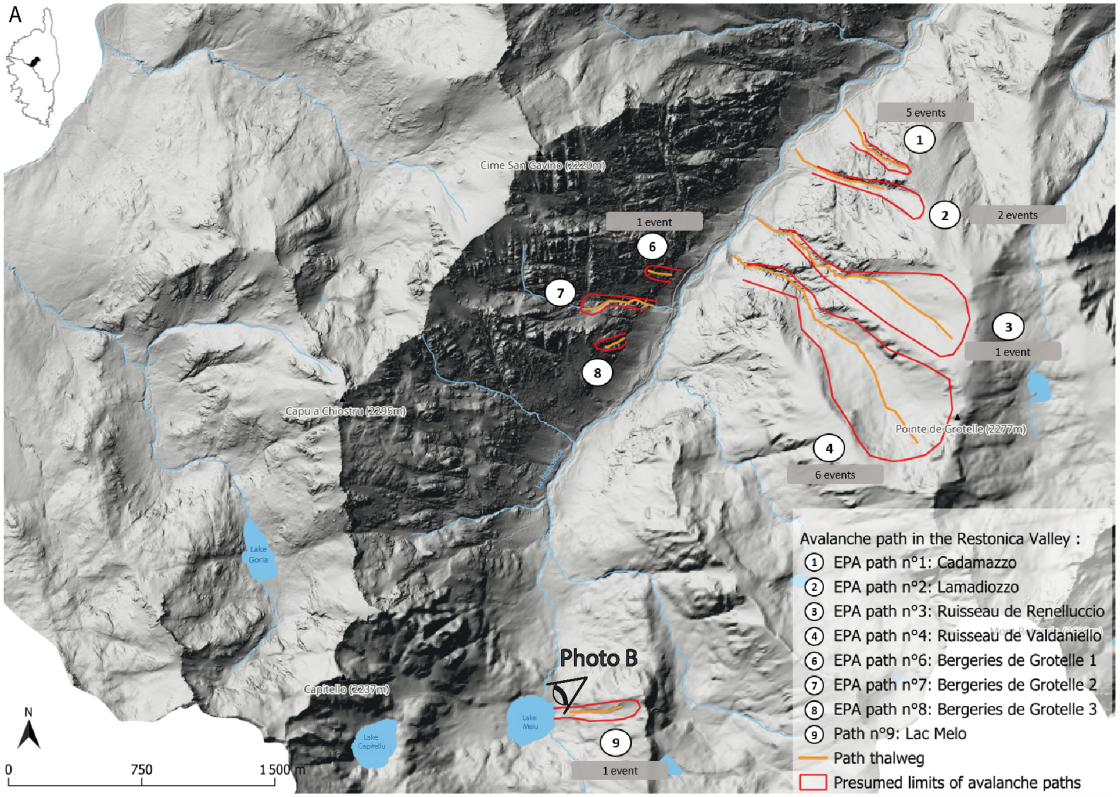



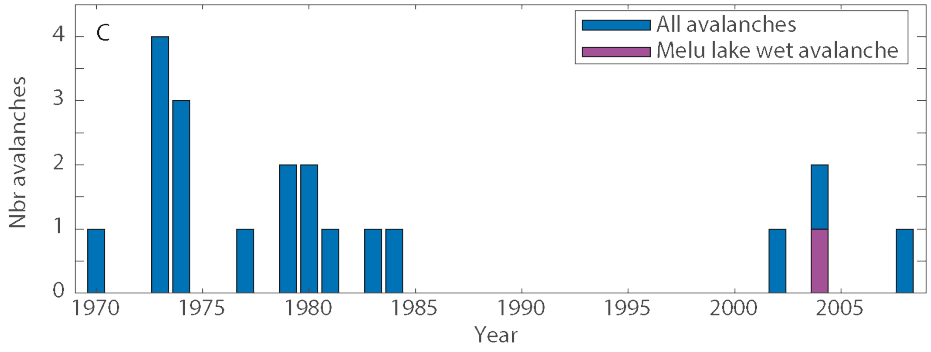


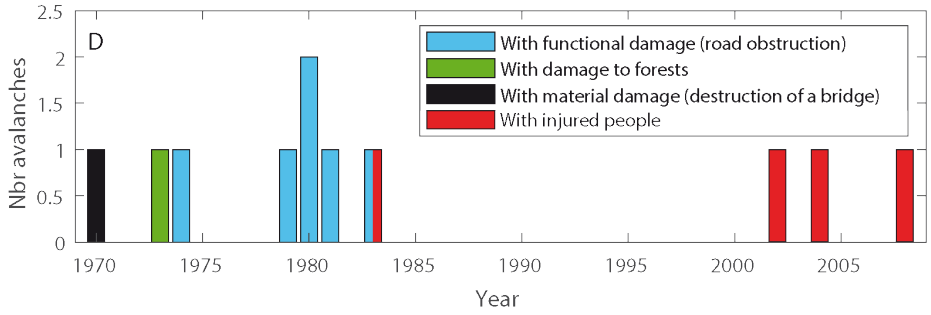


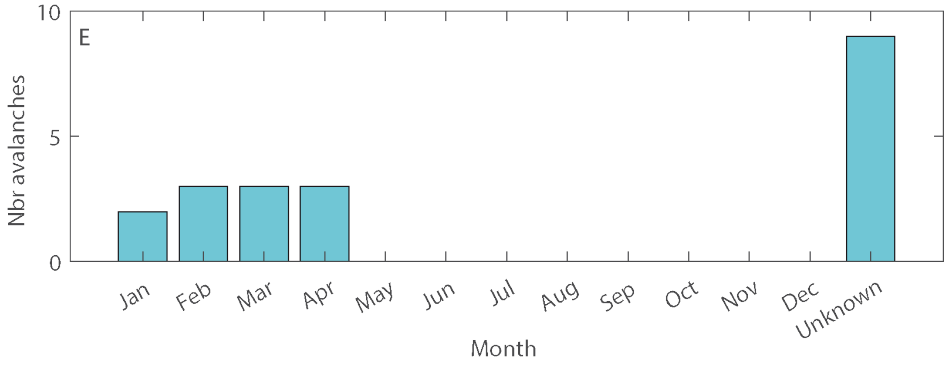


**Figure 6 |** Avalanche observations in the Upper Restonica Valley. A) Avalanche paths where avalanches have been observed. B) Melu Lake on 4 April 2004, see picture location on A). An avalanche occurred during early March, and marks of its impact were still visible one month later (breakage of the ice coverage, presence of sediment and ground), picture S. Guardiola. Chronology of the observed avalanches: C) all avalanches, D) human damage and other damage, and E) seasonal distribution.

Among the 20 avalanches (Figure 6C), 13 had consequences for one or several elements at risk: people, buildings and infrastructures, forests and/or the road network (functional damage). Four avalanches were triggered by skiers, hikers and horseshoe practitioners. This led to three injured people and 1 casualty. Other consequences were limited: 1 avalanche destroyed a bridge, two avalanches broke small pieces of forest, and 7 avalanches reached a road downslope with little functional damage (short obstructions) (Figure 6D).

From a temporal perspective, the 20 avalanches all occurred between the winters of 1970/71 and 2008/09, with zero to 4 avalanches per winter (Figure 6C). More precisely, 16 avalanches occurred between the winters of 1970/71 and 1984/85. All of these except two avalanches were documented by the EPA. Additionally, all of these events, with the exception of the avalanche of early March 1985 which led to one casualty, did not have any consequences for people, but they caused slight damage to roads, forests and bridges. The four other avalanches all occurred

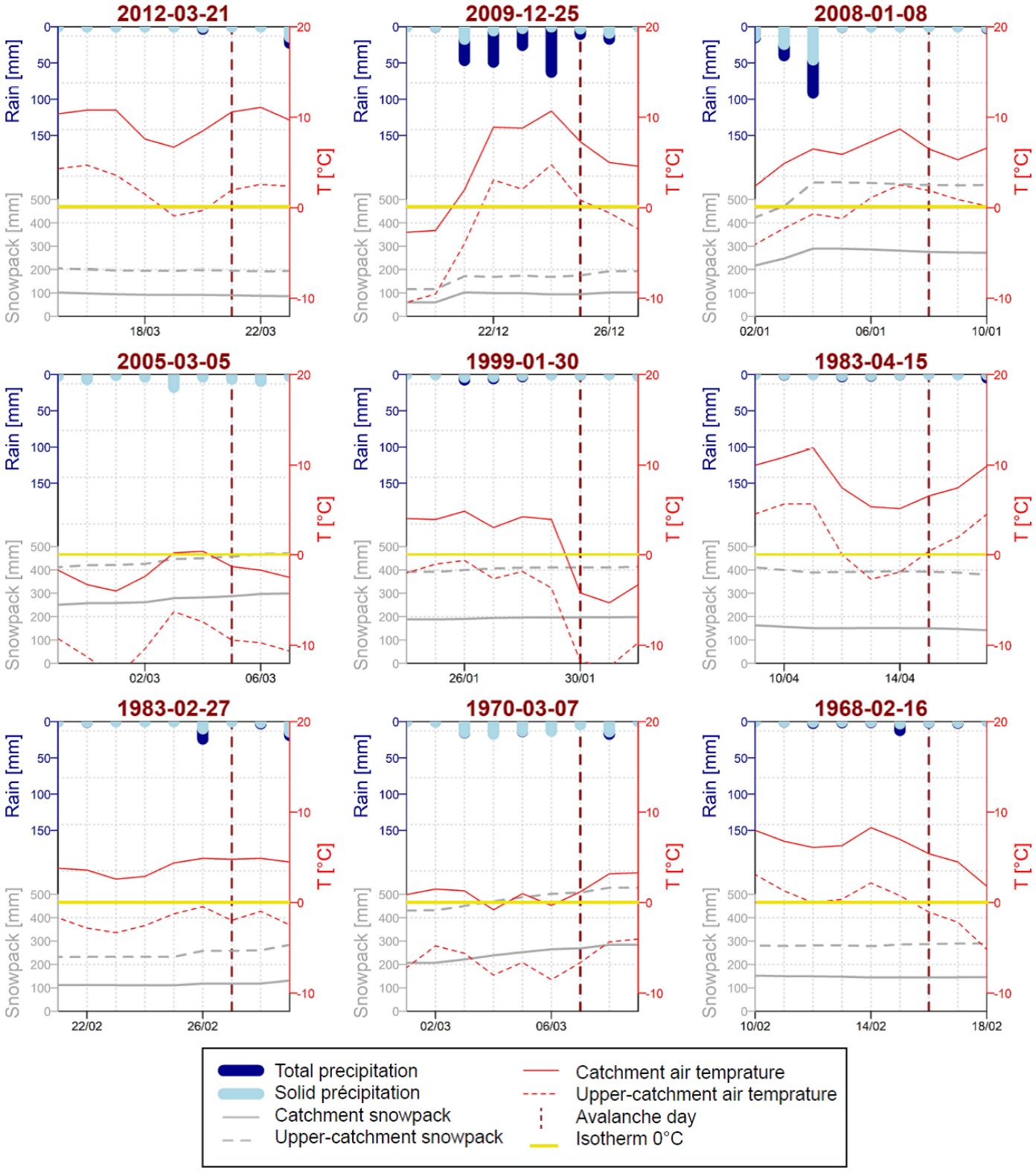


**Figure 7 |** Hydrometeorological reconstitutions of the snow and weather conditions corresponding to the 9 recent avalanches observed over the recent period.

between 2002/03 and 2008/09. In contrast to those of the previous period, none of them were recorded by the EPA. Two avalanches were retrieved from accident reports from the ANENA: 1 was reported by a local technician from meteorological and state services, and one was from a participatory source https://www.data-avalanche.org/. Among these four avalanches, three were accidental triggers leading to 1–2 injured people, and no other damage occurred (Figure 6D). All avalanches for which the date was documented occurred between January and April, and only March 2005 reached Melu Lake (Figure 6E).

### 4.6. Hydrometeorological conditions of recent avalanches

The GR4J and CemaNeige models provide good representations of the hydrological balance of the catchment over the calibration period, with a KGE criterion of 0.75 (this criterion ranges from inferior to 1, with a perfect model having a KGE equal to 1; Brigode et al. (in review) obtained a median KGE criterion of 0.78 when calibrating the same rainfall-runoff model over 130 Mediterranean catchments).

Figure 7 presents the reconstruction of hydrometeorological conditions observed during the 9 recent avalanches for which the precise dates of occurrence (i.e., year, month, and day) are available. The figure depicts the temporal evolution of the snowpack (for both the entire catchment and the upper part of the catchment), air temperature (for both the entire catchment and the upper part of the catchment), and precipitation (total and solid) for the entire catchment, 6 days before and 2 days after the avalanche date.

Some avalanches were observed after a period of increasing air temperature and a rainfall episode (e.g., March 2012, December 2009, February 1983), whereas others were observed following a cooling trend (e.g., January 1999 and February 1968). Therefore, this analysis does not identify common triggering factors for all avalanches. However, all those that occurred between the end of February and April (March 2005, March 2012, the end of February 1983, April 1983, and March 1970) presented a coherent climatic pattern, namely, an increase in snow accumulation or rainfall on snow within the context of a temperature increase. These conditions suggest that these avalanches involved wet snow, as was the case for the one that reached Melu Lake in March 2004 (Figure 6B).

## 5. Discussion

### 5.1. Event deposit interpretation

Three geochemical endmembers were identified and found to be coherent between the two lakes (Figure 2C, D). The first endmember corresponds to increases in siliciclastic elements (Si, Al, K, Zr, and Ti), which are mainly related to the fine material present in F1 and F3 and correspond to terrigenous input from the catchment or from African dust deposition (Sabatier et al., 2020), whereas F1 is also influenced by the third endmember with high Br content. The African dust nature of the finer sediment fraction of this lake sediment is supported by the high amount of palygorskite clay minerals found in Capitellu Lake, with a mean of 10% (data not shown), as found in Bastani Lake (Sabatier et al., 2020). The second endmember, mostly identified in F2, is characterized by a high Rb content and coarse to very coarse sediment originating from the surrounding catchment (granite and related minerals) and was probably rapidly deposited in the lake. The third endmember is enriched in Br, which has a high affinity for organic matter and is related mainly to lake organic matter, and partly influences F1 (Bajard et al., 2016; Lefebvre et al., 2021). The Pb content associated with this third endmember could also complex with organic matter and shows one peak in the upper part of the core between 1950 and 1970 yr cal CE, and another between 1050 and 1200 yr cal CE (Figure 2: black arrows and Figure 5) in CAP13-P3. These two peaks perfectly match known lead pollutions for the Modern and Medieval periods, which were previously observed in Corsica (Sabatier et al., 2020), at the scale of the western Mediterranean area (Elbaz–Poulichet et al., 2011) and in the Alps (Elbaz–Poulichet et al., 2020).

From sedimentary and geochemical data, F1 appears to correspond to background sedimentation characterized by in-lake organic matter and fine terrigenous inputs, whereas F2 and F3 correspond to event deposits in relation to high detrital input, coarser materials or graded beds (Sabatier et al., 2022).

F3 is defined as a normally graded layer with a clay cap and, for some deposits, a coarser base. This graded characteristic is also observed for the Rb associated with coarser grains, which decreases, and the Fe associated with finer grains, which increases in geochemical data from the thicker F3 deposit in Melu (Figure 2B). These deposits are recorded in whole cores and are well correlated in both lakes. The grain size data from these F3 deposits reveal a linear relationship between D50 and D90 (Passega diagram, Figure 3A, C), which indicates the same transport mechanism in relation to the underwater current (Passega, 1964). In terms of geochemistry, F1 and F3 present similar patterns (Figure 2C, D), which probably indicate that F3 corresponds to previously deposited sediment (F1) and then reworked in the lake through the turbiditic current, as suggested by their graded pattern and trajectory in the Passega diagram. Flood deposits do not seem to occur in such lakes with very limited fine sediment material in the catchments, due to very restricted (Melu) to no (Capitellu) river systems. However, the graded characteristics of such deposits involve flow transport, and debris flows cannot be completely ruled out (Kiefer et al., 2021), even if the geochemistry of background sedimentation (F1) and such graded event deposits (F3) mainly support an in situ

reworked origin, which is probably related to an earthquake. The most recent F3 deposit was deposited at 1790 yr cal CE (1720–1903) and at 1753 yr cal CE (1727–1781) on MEL13P3 and CAP13P3, respectively. If F3 is related to a recent earthquake, on the basis of the ESTI (earthquake sensitivity threshold index) developed by Wilhelm et al. (2016), we can estimate which historical earthquake may have induced greater destabilization in the lake. From the diagram based on the plot of the epicentral MSK intensity versus the distance between the lake and the epicenter in the SISFRANCE database (Figure S2), two earthquakes present characteristics (magnitude and lake epicentral distance) for a potentially recorded event: the 1775 CE Vico earthquake (Corsica) and the 1887 CE Imperia earthquake (Italia) (Figure S2). From that method, we can infer that the 1775 CE Vico earthquake corresponded to the stronger earthquake at the lake location and perfectly matched the age of this event from the age model, allowing us to interpret the younger F3 as an earthquake-induced deposit. This earthquake is not well documented but corresponds to the strongest historical earthquake in Corsica (Jomard et al., 2022). In Melu Lake, this event was also characterized by a sandy base enriched in organic matter debris (Figure 2B), which corresponds to the material found on the small delta in the western part of the lake (Figure 1C) and probably indicates a subaqueous landslide from this part of the lake in relation to this earthquake event. In CAP13P3, we record 7 F3 deposits, which could thus be interpreted as earthquake-related deposits, as grain size characteristics present the same trend as the younger F3 deposits in the passega diagram, thus involving the same earthquake trigger (Figure 3). In addition to the 1775 CE Vico event, we recorded 6 earthquakes—1700 (1740–1665), 1320 (1375–1255), 1110 (1170–1005), 755 (850–645), 640 (750–535) and 630 (740–525) yr cal CE—with a mean return period of approximately 200 ±140 yr, but these events seemed to have occurred in 3 clusters of approximately 350 yr. Unfortunately, no older historical earthquakes were documented in Corsica to confirm a local source for all these events.

The F2 deposit is composed of coarse to very coarse rock fragments (gravel) in both lakes, and associated with terrestrial organic remains in Melu (Figure 2A, B). Based on the thickness evolution of F2 event deposits (thicker in the closer core from terrestrial inputs), the core correlations indicate that the source of material for F2 was probably the southwestern part of the Capitellu catchment and the eastern part of the Melu catchment, both of which correspond to the main avalanche corridors (Figure 1B, C). Additionally, grain size data indicate very poor sorting and not grading in such deposits (Figure 3B, D), with organic-rich debris characteristic of avalanche deposits (Fouinat et al., 2017; Nesje et al., 2007; Seierstad et al., 2002; Vasskog et al., 2011). As no grading or coarse material is observed in this F2 event, flooding triggered by high-precipitation events and related hyperpycnal or homopycnal currents can be ruled out (Sabatier et al., 2022). Given that such event deposits consist of coarser material and terrestrial organic matter, debris flow-related processes could be involved. In lake sediment, a debris flow event is characterized by a sharp base of sand-sized sediment with gravel, fining upward to silt with relatively high terrestrial organic matter content, depending on the landscape context (Irmler et al., 2006; Kiefer et al., 2021; Sletten et al., 2003). However, once again, as no grading in relation to underwater current is observed in F2 deposits, we can also exclude debris flow processes. As the F2-type event deposits in the two Corsican lakes present all the characteristics of wet avalanche deposits described in the literature, we conclude that this is the main triggering process. During an avalanche, sediment is carried downslope by rapidly flowing water-saturated snow, and the process of integration into lacustrine sediments depends on whether the lake surface is frozen or not frozen (Sabatier et al., 2022). In the case of a frozen lake, wet avalanches, which are more effective erosional agents than winter dry snow avalanches (Moore et al., 2013), induce deposits in a restricted area on the lake surface close to the avalanche corridor. This material spreads across a large part of the lake by drifting ice during melting, and coarse particles drop to the lake floor, which induces dropstones in the sediment (Thys et al., 2019). If an avalanche occurs when the lake is ice free or possibly breaks the ice when it reaches the lake, the avalanche material directly enters the water, and then, the particles are concentrated in a more restricted area closer to the avalanche corridor and then observed as a gravel-rich layer in the sediment (Sabatier et al., 2022). Some small dropstones are observed in the F1 sediment of both lakes, but are more frequent in F2 and correspond to a specific layer enriched in gravel and organic matter, which favors the second mechanism described above.

The youngest F2 deposit in MEL13P3 is between 31 and 36 mm thick and is not recorded in the MEL13P2 core (Figure 2B) dated through short-lived radionuclides (Figure 4B). However, from the XRF-based correlation, this event could be dated to 2004.7 ± 1.5 years owing to the MEL13P2 chronology (Figure 2B). This dated 5 mm event could be attributed to the 05.03.2005 wet avalanche identified via photography in Melu Lake (Figure 6B), which is another strong argument for the identification of F2 as a wet avalanche deposit. Before the 2005 wet avalanche deposit, the previous event in Melu Lake was dated between 1973 and 1985 and may have corresponded to one of the 15 avalanche events recorded in the EPA during this period (Figure 6C). If we consider avalanches solely from the end of February to April (wet avalanches), 8 of these 15 events could correspond, and only one of them (05.05.1985) is potentially identified around Melu Lake, however without a precise location. These historical versus lake sediment comparisons indicate that most EPA events in the Restonica Valley are not recorded in Melu/Capitellu Lakes. However, the two phases of increased wet avalanche frequency in the EPA record (around 2005 and around 1980) correspond to the two upper avalanche deposit ages recorded in lake sediments (Figure 6C); thus,

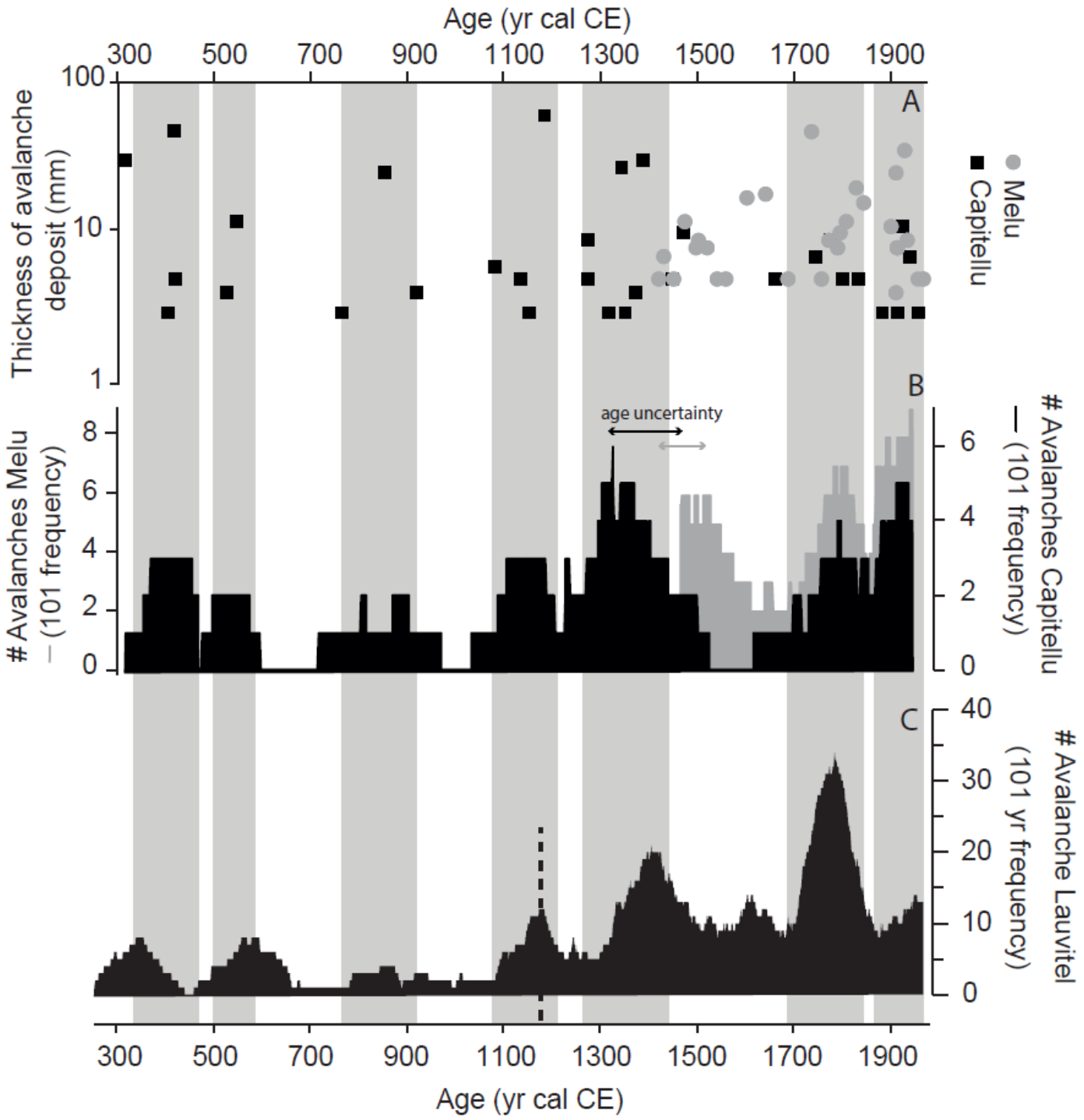


**Figure 8 |** Wet avalanche records from the Melu (gray) and Capitellu (black) Lakes. A) Thickness of each wet avalanche deposit, B) 101-yr avalanche frequency and C) Ecrins Massif wet avalanche chronicle, where the dashed black line represents a main shift in wet avalanche chronicle due to forest clearance (Fouinat et al., 2018). The vertical band represents a common increase in wet avalanche frequency in both massifs. The double arrows in part B indicate age model uncertainties for each chronicle.

we conclude that these lakes could be interpreted as wet avalanche chronicles.

### 5.2. Resulting avalanche chronicles

Owing to the interpretation of F2 as wet avalanche deposits associated with the age model (Figure 5), we can produce sediment base records for the two lakes (Figure 8). These records cover the last 580 and 1700 yr for Melu and Capitellu Lakes, respectively, and allow a direct comparison of these two records over approximately 600 years. To produce a wet avalanche chronicle, we used a 101-year running sum, which more or less integrates the age model uncertainties (Figure 8B). Since 1700 yr cal CE, the two periods presented the same variation, with higher frequencies in 1970–1885 and 1860–1715 and lower frequencies in between. The shorter record in Melu does not allow a direct comparison of the older period of frequency increase before 1600 yr cal CE, even if it shows a frequency increase that could be compared to that observed

in Capitellu before 1540 yr cal CE (Figure 8B). The Melu chronicle presents a relatively high frequency of avalanche deposits, but both chronicles are in good agreement with the synchronous avalanche variations within age model uncertainties (Figure 8), which supports our interpretation of a common wet avalanche trigger process. In terms of avalanche deposit thickness, thicker deposits are present before 1400 yr cal CE in the Capitellu chronicle, but for the recovery period after 1430 yr cal CE, the comparison of both records seems to indicate that thicker deposits occurred in the same period in both lakes (Figure 8A). The avalanche period from Capitellu Lake allows the identification of 7 periods of frequency increase: 1970–1885, 1860–1715, 1515–1280, 1215–1095, 910–820, 575–500 and 370–470 yr cal CE (Figure 8).

The meteorological conditions favorable for wet avalanche releases include 1) the loss of strength by water infiltration, 2) the thickening of wet snowpack by snow precipitation, and 3) the warming of snowpack above 0°C (Baggi & Schweizer, 2009). More broadly, the involvement of wet snow within avalanche flows implies mild weather conditions. The reconstruction of the snow and weather conditions that prevailed when avalanches from the Corsican EPA occurred revealed that those from the end of February to April (Figure 6C) were likely wet snow avalanches, as they occurred after a rain-on-snow event and/or a temperature increase (Figure 7). This information confirms the rather strenuous wet snow avalanche activity in the upper Restonica, making lake sediments an efficient proxy.

### 5.3. Avalanche chronicles comparison

In the Queyras massif (southeast French Alps), on the basis of tree ring series, 38 destructive snow avalanches were identified between 1338 and 2010 (Corona et al., 2013), which were recently extended by Favillier et al. (2023b), with three avalanche activity periods increasing between 1645-–1715, 1790–1830 and 1959–1987 (Favillier et al., 2023b). The two later periods correspond rather well to the higher wet avalanche frequency in Corsica identified in our lake records (Figure 8B).

A unique wet avalanche chronicle similar to ours in Western Europe was published by Fouinat et al. (2018) in Lake Lautivel sediment, a lake at 1500 m a.s.l. in the Ecrins Massif in the Alps, approximately 400 km north of the studied area. The Lauvitel avalanche chronicle presented a significant change at 1170 yr cal. CE (Figure 8C), potentially related to changes in vegetation cover (forest clearance by human activity), which resulted in increased wet avalanche frequency in this area (Fouinat et al., 2018). Such a pattern is not recorded in the Monte Ritondu Massif, as no shift in wet avalanche frequency is detected, and the signal seems relatively stable over time with frequency variation. but no obvious tipping point (Figure 8B). A comparison of the 101-year avalanche frequency in the Monte Ritondu and Ecrins massifs, however, revealed that the frequency increased during the same period for the 7 identified episodes of high wet avalanche frequency (Figure 8). This synchronicity confirms the consistency of the reconstructed chronicles and suggests potential common climate forcing in both massifs over this period.

Eckert et al. (2013) describe EPA data from the French Alps from 1946 and 2010, and show that avalanche occurrences between the northern and southern French Alps are partially coupled. In the north, winter snow depth seems to be the main control parameter, whereas in the south, there is better correlation with temperature in the southern Alps. Moreover, the decreasing trend in avalanche numbers, coupled with the increasing trend in avalanche means and high-magnitude runout elevations for the late 20$^{th}$ century, corresponds to a period of marked warming (Eckert et al., 2013). Owing to its different resolutions, the reconstructed Corsica avalanche chronicle is not directly comparable with these results. However, the in-phase variability of wet avalanches in the Corsica and Ecrins massifs (Figure 8B, C) may be related to the partial coupling between avalanche activity in the northern and southern French Alps. Furthermore, the main tipping point observed in the French Alps since 1980/85, with a significant upslope retreat of large avalanches (Eckert et al., 2013), is consistent with the fact that just one avalanche was recorded until approximately 1965 in the Corsican lakes.

An increase in wet snow avalanche activity (at least in terms of proportion with respect to dry snow avalanches) has been documented in different records (Pielmeier et al., 2013; Eckert et al., 2024) and notably in some massifs of the French Alps over recent decades (Naaim et al., 2016; Reuter et al., 2025), and such trends are expected to continue with future climate warming (Mayer et al., 2024; Eckert et al., 2024). Despite the very different time scales of our records, the increase we document over the most recent period of our analysis is consistent with this ongoing evolution. In addition, it puts it in a longer perspective, showing that previous periods of increase and decrease have existed for centuries.

All methodologies used to acquire data on past avalanche activity have their own weaknesses (Eckert et al., 2024). Many studies rely on systematic avalanche observations or historical archives that provide large records of different types of avalanches (e.g., wet and dry) and often additional information such as size and damage. However, acquiring such data is time consuming and costly, and most available series (at least instrumental series) are too short to understand the long-term climate impact at centennial time scales. Additionally, chronologies resulting from such sources are often strongly shaped by sources (Fig. 6C, D), which precludes inferring changes in risks and hazards without careful data analysis (Giacona et al., 2019). A popular alternative for reconstructing series of past avalanches is dendrogeomorphology, leading chronologies of annual resolution; however, this approach

is limited by the presence of trees in avalanche paths, and chronologies are generally restricted to 1–3 centuries, with a decrease in efficiency as one moves further back in the past (Favillier et al., 2023b). Here, with an innovative combination of methods (lake sediment and avalanche observations with weather analyses), we confirm the usefulness of a paleolimnological approach even if it records only wet avalanche events that reach the lake surface and are powerful enough to transport a sufficient amount of material. This method also has several limitations in terms of 1) the possibility of recording only wet avalanches linked to high amounts of transported materials, 2) the low temporal resolution with chronological uncertainties, 3) the ability to perform deep sedimentological and geochemical analyses to identify wet avalanche deposits among other potential triggers (floods, debris flows, earthquakes), and 4) the ability to record only wet avalanche events from avalanche paths reaching the lake; thus, spatial coverage is less important than other methods. Given these limitations, the produced chronicles, especially from two neighboring lake sediments even at relatively low resolutions, seem to be representative of the centennial to millennial wet avalanche frequency of the valley. Hence, the approach may be useful for tracking changes in avalanche activity and related risks in mountainous areas where few data are available. Furthermore, the combination of different data sources may provide an excellent perspective to reach long records as exhaustively as possible in the future, combining the strength of each approach to compensate for the weaknesses of each of them.

## 6. Conclusions

Within the context of rapidly evolving mountain hazards and related risks, being able to assess how they have changed over long time scales is crucial. However, for snow avalanches, classical time series exceeding a few decades are rare, and records covering more than 2–3 centuries are exceptional. In this study, we developed a comprehensive methodology associated with two neighboring lake sediment records, observed data sources related to past avalanches, and reconstructions of snow and weather patterns corresponding to their dates of occurrence.

We first identify the sedimentary facies characteristics of wet avalanche deposits and validate this attribution using historical data via a well-defined age model. The two records are in good agreement with the synchronous avalanche variations within the age model uncertainties. Compared with historical snow avalanches and weather analyses, this novel methodology allows us to reconstruct 1700-year-long chronicles of wet snow deposits from lake sediments in Corsica, demonstrating their linkages with local archives, as well as regional patterns in wet avalanche frequency, which can be useful for anticipating changes and related risks in Corsica.

These results further demonstrate the interest of lake sediment as a natural archive for capturing wet avalanche frequency patterns over long time frames and as an additional data source to those generally considered: systematic observations, historical sources, and tree rings. New approaches to mitigate avalanche risk and design efficient adaptation strategies that explicitly account for changes in activity patterns are needed (Eckert and Giacona, 2023). This especially applies in areas that have seen little research efforts; hence, this novel methodological approach, which is based on paleolimnological studies, alone or combined with other avalanche data sources, may be useful for tracking changes in avalanche activity and related risks in mountainous areas.

## Acknowledgements

We thank the Parc Naturel Regional de Corse, the Direction Regionale de l'Environnement, de l'Aménagement et du Logement de Corse (DREAL) and the Office de l'Environnement de la Corse (OEC; Gwenaëlle Baldovini and Pierre-Jean Albertini) for their coring authorization and support during fieldwork. The authors would like to thank Jérôme Debret for his help during the field trip. 14C analyses were performed with the aid of the CNRS-INSU ARTEMIS national radiocarbon AMS measurement program at Laboratoire de Mesure 14C (LMC14) at the CEA Institute at Saclay (French Atomic Energy Commission). The authors would also like to thank the Laboratoire Souterrain de Modane (LSM) facilities for the gamma spectrometry measurements EDYTEM for the X-ray fluorescence analyses. A. Bisquert, N. Eckert and F. Giacona are members of the Grenoble Risk Institute (https://risk.univ-grenoble-alpes.fr). They acknowledge support from the French National Research Agency to the IRIMONT program (ANR-22-EXIR-0003). EDYTEM and IGE are members of Labex OSUG. This research was supported by Culletivittà di Corsica through the GERHYCO interdisciplinary project dedicated to water management, ecology and hydroecosystem services in the island context..

## Author contribution

PS and BV designed the study, PS, MaD, YC, EM, JD, BV collected data from both lakes, VB, MK, MCB acquiered data on lake sediments, AB, NE, FG, MiD work on the historical avalanche data, PB analyses hydrometerological data, FH, EG fund a part of the analyses, PS wrote the manuscript with input from all co-authors

## Data availability

The data is available from Zenodo at https://doi.org/10.5281/zenodo.17491191

## Conflict of interest

The authors declare that they have no known competing financial interests or personal relationships that could have appeared to influence the work reported in this paper..

## References


Baggi, S., Schweizer, J. (2009). Characteristics of wet-snow avalanche activity: 20 years of observations from a high alpine valley (Dischma, Switzerland). Natural Hazards 50(1), 97–108. https://doi.org/10.1007/s11069-008-9322-7

Bajard, M., Sabatier, P., David, F., Develle, A.-L., Reyss, J.-L., Fanget, B., Malet, E., Arnaud, D., Augustin, L., Crouzet, C., Poulenard, J., Arnaud, F. (2016). Erosion record in Lake La Thuile sediments (Prealps, France): Evidence of montane landscape dynamics throughout the Holocene. The Holocene 26(3), 350–364. https://doi.org/10.1177/0959683615609750

Beniston, M., Farinotti, D., Stoffel, M., Andreassen, L.M., Coppola, E., Eckert, N., Fantini, A., Giacona, F., Hauck, C., Huss, M., Huwald, H., Lehning, M., López-Moreno, J.-I., Magnusson, J., Marty, C., Morán-Tejéda, E., Morin, S., Naaim, M., Provenzale, A., Rabatel, A., Six, D., Stötter, J., Strasser, U., Terzago, S., Vincent, C. (2018). The European mountain cryosphere: a review of its current state, trends, and future challenges. The Cryosphere 12(2), 759–794. https://doi.org/10.5194/tc-12-759-2018

Blaauw, M. (2010). Methods and code for 'classical' age-modelling of radiocarbon sequences. Quaternary Geochronology, 5(5), 512–518. https://doi.org/10.1016/j.quageo.2010.01.002

Blott, S.J., Pye, K. (2001). GRADISTAT: a grain size distribution and statistics package for the analysis of unconsolidated sediments. Earth Surface Processes and Landforms, 26(11), 1237–1248. https://doi.org/10.1002/esp.261

Bourova, E., Maldonado, E., Leroy, J. B., Alouani, R., Eckert, N., Bonnefoy-Demongeot, M., & Deschatres, M. (2016). A new web-based system to improve the monitoring of snow avalanche hazard in France. Natural Hazards and Earth System Sciences, 16(5), 1205-1216. https://doi.org/10.5194/nhess-16-1205-2016

Brigode, P., Brissette, F., Nicault, A., Perreault, L., Kuentz, A., Mathevet, T., Gailhard, J. (2016). Streamflow variability over the 1881–2011 period in northern Québec: comparison of hydrological reconstructions based on tree rings and geopotential heightfield reanalysis. Climate of the Past, 12(9), 1785–1804. https://doi.org/10.5194/cp-12-1785-2016

Brigode, P., & Oudin, L. (2024). Using Global Reanalysis and Rainfall-Runoff Model to Study Multi-Decadal Variability in Catchment Hydrology at the European Scale. Hydrology and Earth System Sciences Discussions, 1 30. https://doi.org/10.5194/hess-2024-336

Bruel, R., Sabatier, P. (2020). serac: an R package for ShortlivEd RAdionuclide chronology of recent sediment cores. Journal of Environmental Radioactivity 225, 106449. https://doi.org/10.1016/j.jenvrad.2020.106449

Castebrunet, H., Eckert, N., Giraud, G., Durand, Y., Morin, S. (2014). Projected changes of snow conditions and avalanche activity in a warming climate: the French Alps over the 2020–2050 and 2070–2100 periods. The Cryosphere 8(5), 1673–1697. https://doi.org/10.5194/tc-8-1673-2014

Coron, L., Thirel, G., Delaigue, O., Perrin, C. and Andréassian, V. (2017). The Suite of Lumped GR Hydrological Models in an R package. Environmental Modelling and Software, 94, 166-171, https://doi.org/ 10.1016/j.envsoft.2017.05.002

Coron, L., Delaigue, O., Thirel, G., Dorchies, D., Perrin, C. and Michel, C. (2022). airGR: Suite of GR Hydrological Models for Precipitation-Runoff Modelling. R package version 1.7.0, https://doi.org/10.15454/EX11NA, URL: https://CRAN.R-project.org/package=airGR

Corona, C., Rovéra, G., Lopez Saez, J., Stoffel, M., Perfettini, P. (2010). Spatio-temporal reconstruction of snow avalanche activity using tree rings: Pierres Jean Jeanne avalanche talus, Massif de l'Oisans, France. Catena 83(2-3), 107–118. https://doi.org/10.1016/j.catena.2010.08.004

Corona, C., Saez, J.L., Stoffel, M., Rovéra, G., Edouard, J.-L., Berger, F. (2013). Seven centuries of avalanche activity at Echalp (Queyras massif, southern French Alps) as inferred from tree rings. The Holocene 23(2), 292–304. https://doi.org/10.1177/0959683612460784

Durand, Y., Giraud, G., Laternser, M., Etchevers, P., Mérindol, L., & Lesaffre, B. (2009). Reanalysis of 47 years of climate in the French Alps (1958–2005): climatology and trends for snow cover. Journal of applied meteorology and climatology, 48(12), 2487-2512. https://doi.org/10.1175/2009JAMC1810.1

Eckert, N., Baya, H., Deschatres, M. (2010). Assessing the Response of Snow Avalanche Runout Altitudes to Climate Fluctuations Using Hierarchical Modeling: Application to 61 Winters of Data in France. Journal of Climate 23(12), 3157–3180. https://doi.org/10.1175/2010JCLI3312.1

Eckert, N., Keylock, C.J., Castebrunet, H., Lavigne, A., Naaim, M. (2013). Temporal trends in avalanche activity in the French Alps and subregions: from occurrences and runout altitudes to unsteady return periods. Journal of Glaciology, 59(213), 93–114. https://doi.org/10.3189/2013JoG12J091

Eckert, N., & Giacona, F. (2023). Towards a holistic paradigm for long-term snow avalanche risk assessment and mitigation. Ambio, 52(4), 711-732. https://doi.org/10.1007/s13280-022-01804-1

Eckert, N., Corona, C., Giacona, F., Gaume, J., Mayer, S., van Herwijnen, A., Hagenmuller, P., & Stoffel, M. (2024). Climate change impacts on snow avalanche activity and related risks. Nature Reviews Earth & Environment, 1-21. https://doi.org/10.1038/s43017-024-00540-2

Elbaz-Poulichet, F., Dezileau, L., Freydier, R., Cossa, D., Sabatier, P. (2011). A 3500-Year Record of Hg and Pb Contamination in a Mediterranean Sedimentary Archive (The Pierre Blanche Lagoon, France). Environmental Science & Technology 45(20), 8642–8647. https://doi.org/10.1021/es2004599

Elbaz-Poulichet, F., Guédron, S., Anne-Lise, D., Freydier, R., Perrot, V., Rossi, M., Piot, C., Delpoux, S., Sabatier, P. (2020). A 10,000-year record of trace metal and metalloid (Cu, Hg, Sb, Pb) deposition in a western Alpine lake (Lake Robert, France): Deciphering local and regional mining contamination. Quaternary Science Reviews 228, 106076. https://doi.org/10.1016/j.quascirev.2019.106076

Favillier, A., Guillet, S., Trappmann, D., Morel, P., Lopez-Saez, J., Eckert, N., Zenhäusern, G., Peiry, J.-L., Stoffel, M., & Corona, C. (2018). Spatio-temporal maps of past avalanche events derived from tree-ring analysis: A case study in the Zermatt valley (Valais, Switzerland). Cold Regions Science and Technology, 154, 9-22. https://doi.org/10.1016/j.coldregions.2018.06.004

Favillier, A., Guillet, S., Lopez-Saez, J., Giacona, F., Eckert, N., Zenhäusern, G., Peiry, J. L., Stoffel, M., & Corona, C. (2023). Identifying and interpreting regional signals in tree-ring based reconstructions of snow avalanche activity in the Goms valley

(Swiss Alps). Quaternary Science Reviews, 307, 108063. https://doi.org/10.1016/j.quascirev.2023.108063

Favillier, A., Eckert, N., Lopez-Saez, J, Stoffel, M., Corona, C. (2023b). Effects of Climate Change on snow avalanche activity in the alps: insights from a 456-year tree-ring derived chronology in the Queyras massif (France). In Proceedings, International Snow Science Workshop. Bend, Oregon. p. 6.

Fouinat, L., Sabatier, P., David, F., Montet, X., Schoeneich, P., Chaumillon, E., Poulenard, J., Arnaud, F. (2018). Wet avalanches: long-term evolution in the Western Alps under climate and human forcing. Climate of the Past 14(9), 1299–1313. https://doi.org/10.5194/cp-14-1299-2018

Fouinat, L., Sabatier, P., Poulenard, J., Reyss, J.-L., Montet, X., Arnaud, F. (2017). A new CT scan methodology to characterize a small aggregation gravel clast contained in a soft sediment matrix. Earth Surface Dynamics 5(1), 199–209. https://doi.org/10.5194/esurf-5-199-2017

Gagnon-Poiré, A., Brigode, P., Francus, P., Fortin, D., Lajeunesse, P., Dorion, H., Trottier, A.-P. (2021). Reconstructing past hydrology of eastern Canadian boreal catchments using clastic varved sediments and hydro-climatic modelling: 160 years of fluvial inflows. Climate Of the Past Discussions, 17(2), 653–673. https://doi.org/10.5194/cp-17-653-2021

Gaume, J., Chambon, G., Eckert, N., Naaim, M. (2012). Relative influence of mechanical and meteorological factors on avalanche release depth distributions: An application to French Alps. Geophysical Research Letters 39(12), 2012GL051917. https://doi.org/10.1029/2012GL051917

Giacona, F., Eckert, N., & Martin, B. (2017a). La construction du risque au prisme territorial: dans l'ombre de l'archétype alpin, les avalanches oubliées de moyenne montagne. Natures sciences sociétés, 25(2), 148-162. https://doi.org/10.1051/nss/2017025

Giacona, F., Eckert, N., & Martin, B. (2017b). A 240-year history of avalanche risk in the Vosges Mountains based on non-conventional (re) sources. Natural Hazards and Earth System Sciences, 17(6), 887-904. https://doi.org/10.5194/nhess-17-887-2017

Giacona, F., Martin, B., Eckert, N., & Desarthe, J. (2019). Une méthodologie de la modélisation en géohistoire: de la chronologie (spatialisée) des événements au fonctionnement du système par la mise en correspondance spatiale et temporelle. Physio-Géo. Géographie physique et environnement, (Volume 14), 171-199. https://doi.org/10.4000/physio-geo.9186

Giacona, F., Eckert, N., Corona, C., Mainieri, R., Morin, S., Stoffel, M., Martin, B., Naaim, M. (2021). Upslope migration of snow avalanches in a warming climate. Proceedings of the National Academy Of Sciences 118(44), e2107306118. https://doi.org/10.1073/pnas.2107306118

Gupta, H.V., Kling, H., Yilmaz, K.K., Martinez, G.F. (2009). Decomposition of the mean squared error and NSE performance criteria: Implications for improving hydrological modelling. Journal of Hydrology 377(1-2), 80–91. https://doi.org/10.1016/j.jhydrol.2009.08.003

Hao, J., Zhang, X., Cui, P., Li, L., Wang, Y., Zhang, G., Li, C. (2023). Impacts of Climate Change on Snow Avalanche Activity Along a Transportation Corridor in the Tianshan Mountains. International Journal of Disaster Risk Science, 14(4), 510–522. https://doi.org/10.1007/s13753-023-00475-0

Heiri, O., Lotter, A.F., Lemcke, G. (2001). Loss on ignition as a method for estimating organic and carbonate content in sediments: reproducibility and comparability of results. Journal of Paleolimnology 25(1), 101–110. https://doi.org/10.1023/A:1008119611481

Irmler, R., Daut, G., and Mäusbacher, R. (2006). A debris flow calendar derived from sediments of lake Lago di Braies (N. Italy), Geomorphology, 77(1-2), 69–78. https://doi.org/10.1016/j.geomorph.2006.01.013

IPCC. (2022). The Ocean and Cryosphere in a Changing Climate: Special Report of the Intergovernmental Panel on Climate Change, 1st ed. Cambridge University Press. https://doi.org/10.1017/9781009157964

Jacquemart, M., Weber, S., Chiarle, M., Chmiel, M., Cicoira, A., Corona, C., Eckert, N., Gaume, J., Giacona, F., Hirschberg, J., Kaitna, R., Magnin, F., Mayer, S., Moos, C., van Herwijnen, A., Stoffel, M. (2024). Detecting the impact of climate change on alpine mass movements in observational records from the European Alps, Earth-Science Reviews, 258, 104886, https://doi.org/10.1016/j.earscirev.2024.104886.

Jomard, H., Scotti, O., Auclair, S., Dominique, P., Manchuel, K., Sicilia, D. (2022). The SISFRANCE database of historical seismicity. State of the art and perspectives. Comptes Rendus. Géoscience 353, 257–280. https://doi.org/10.5802/crgeos.91

Jomelli, V., Bertran, P. (2001). Wet snow avalanche deposits in the french alps: structure and sedimentology. Geografiska Annaler: Series A, Physical Geography 83(1-2), 15–28. https://doi.org/10.1111/j.0435-3676.2001.00141.x

Jomelli, V., Delval, C., Grancher, D., Escande, S., Brunstein, D., Hetu, B., Filion, L., Pech, P. (2007). Probabilistic analysis of recent snow avalanche activity and weather in the French Alps. Cold Regions Science and Technology 47(1-2), 180–192. https://doi.org/10.1016/j.coldregions.2006.08.003

Kiefer, C., Oswald, P., Moernaut, J., Fabbri, S. C., Mayr, C., Strasser, M., and Krautblatter, M. 2021. A 4,000 year debris-flow record based on amphibious investigations of fan delta activity in Plansee (Austria, Eastern Alps), Earth Surface Dynamics, 9, 1481-1503. https://doi.org/10.5194/esurf-9-1481-2021

Laternser, M., Pfister, C. (1997). Avalanches in Switzerland 1500–1990. In Matthews, J.A., Brundsen, D., Frenzel, B., Glaser, B., & weib, M.M. (Eds.), Rapid Mass Movement as a Source of Climatic Evidence for the Holocene, Palaeoclimate Research 19. Fischer, Stuttgart, pp. 241–266.

Lazar, B., Williams, M. (2008). Climate change in western ski areas: Potential changes in the timing of wet avalanches and snow quality for the Aspen ski area in the years 2030 and 2100. Cold Regions Science and Technology 51(2-3), 219–228. https://doi.org/10.1016/j.coldregions.2007.03.015

Le Roux, E., Evin, G., Samacoïts, R., Eckert, N., Blanchet, J., Morin, S. (2023). Projection of snowfall extremes in the French Alps as a function of elevation and global warming level. The Cryosphere 17(11), 4691–4704. https://doi.org/10.5194/tc-17-4691-2023

Lefebvre, P., Sabatier, P., Mangeret, A., Gourgiotis, A., Le Pape, P., Develle, A.-L., Louvat, P., Diez, O., Reyss, J.-L., Gaillardet, J., Cazala, C., Morin, G. (2021). Climate-driven fluxes of organic-bound uranium to an alpine lake over the Holocene. Science of The Total Environment 783, 146878. https://doi.org/10.1016/j.scitotenv.2021.146878

Liu, Y., Liu, X., Sun, Y. (2021). QGrain: An open-source and easy-to-use software for the comprehensive analysis of grain size distributions. Sedimentary Geology 423, 105980. https://doi.org/10.1016/j.sedgeo.2021.105980

Matiu, M., Crespi, A., Bertoldi, G., Carmagnola, C. M., Marty, C., Morin, S., Schöner, W., Cat Berro, D., Chiogna, G., De

Gregorio, L., Kotlarski, S., Majone, B., Resch, G., Terzago, S., Valt, M., Beozzo, W., Cianfarra, P., Gouttevin, I., Marcolini, G., Notarnicola, C., Petitta, M., Scherrer, S. C., Strasser, U., Winkler, M., Zebisch, M., Cicogna, A., Cremonini, R., Debernardi, A., Faletto, M., Gaddo, M., Giovannini, L., Mercalli, L., Soubeyroux, J. M., Sušnik, A., Trenti, A., Urbani, S., & Weilguni, V. (2021). Observed snow depth trends in the European Alps: 1971 to 2019. The Cryosphere, 15(3), 1343-1382. https://doi.org/10.5194/tc-15-1343-2021

Mayer, S., Hendrick, M., Michel, A., Richter, B., Schweizer, J., Wernli, H., & van Herwijnen, A. (2024). Impact of climate change on snow avalanche activity in the Swiss Alps. The Cryosphere, 18(11), 5495-5517. https://doi.org/10.5194/tc-18-5495-2024

Mitterer, C. & Schweizer, J. (2013). Analysis of the snow-atmosphere energy balance during wet-snow instabilities and implications for avalanche prediction. The Cryosphere 7(1), 205–216. https://doi.org/10.5194/tc-7-205-2013

Mock, C.J., Birkeland, K.W. (2000). Snow Avalanche Climatology of the Western United States Mountain Ranges. Bulletin of the American Meteorological Society 81(10), 2367–2392. https://doi.org/10.1175/1520-0477(2000)081<2367:SACOTW>2.3.CO;2

Moore, J.R., Egloff, J., Nagelisen, J., Hunziker, M., Aerne, U., Christen, M. (2013). Sediment Transport and Bedrock Erosion by Wet Snow Avalanches in the Guggigraben, Matter Valley, Switzerland. Arctic, Antarctic, and Alpine Research 45(3), 350–362. https://doi.org/10.1657/1938-4246-45.3.350

Naaim, M., Eckert, N., Giraud, G., Faug, T., Chambon, G., Naaim-Bouvet, F., & Richard, D. (2016). Impact du réchauffement climatique sur l'activité avalancheuse et multiplication des avalanches humides dans les Alpes françaises. La Houille Blanche, (6), 12-20. https://doi.org/10.1051/lhb/2016055

Nesje, A., Bakke, J., Dahl, S.O., Lie, Ø., Bøe, A.-G. (2007). A continuous, high-resolution 8500-yr snow-avalanche record from western Norway. The Holocene 17(2), 269–277. https://doi.org/10.1177/0959683607075855

Passega, R. (1964). Grain size representation by CM patterns as a geologic tool. Journal of Sedimentary Research 34(4), 830–847. https://doi.org/10.1306/74D711A4-2B21-11D7-8648000102C1865D

Perrin, C., Michel, C., Andréassian, V. (2003). Improvement of a parsimonious model for streamflow simulation. Journal of Hydrology 279(1-4), 275–289. https://doi.org/10.1016/S0022-1694(03)00225-7

Pielmeier, C., Techel, F., Marty, C., & Stucki, T. (2013, October). Wet snow avalanche activity in the Swiss Alps–trend analysis for mid-winter season. In Proceedings of the International Snow Science Workshop, Grenoble and Chamonix (pp. 1240-1246).

Rapuc, W., Sabatier, P., Arnaud, F., Palumbo, A., Develle, A.-L., Reyss, J.-L., Augustin, L., Régnier, E., Piccin, A., Chapron, E., Dumoulin, J.-P., von Grafenstein, U. (2019). Holocene-long record of flood frequency in the Southern Alps (Lake Iseo, Italy) under human and climate forcing. Global and Planetary Change 175, 160–172. https://doi.org/10.1016/j.gloplacha.2019.02.010

Reimer, P.J., Austin, W.E.N., Bard, E., Bayliss, A., Blackwell, P.G., Bronk Ramsey, C., Butzin, M., Cheng, H., Edwards, R.L., Friedrich, M., Grootes, P.M., Guilderson, T.P., Hajdas, I., Heaton, T.J., Hogg, A.G., Hughen, K.A., Kromer, B., Manning, S.W., Muscheler, R., Palmer, J.G., Pearson, C., van der Plicht, J., Reimer, R.W., Richards, D.A., Scott, E.M., Southon, J.R., Turney, C.S.M., Wacker, L., Adolphi, F., Büntgen, U., Capano, M., Fahrni, S.M., Fogtmann-Schulz, A., Friedrich, R., Köhler, P., Kudsk, S., Miyake, F., Olsen, J., Reinig, F., Sakamoto, M., Sookdeo, A., Talamo, S. (2020). The IntCal20 Northern Hemisphere Radiocarbon Age Calibration Curve (0–55 cal kBP). Radiocarbon 62(4), 725–757. https://doi.org/10.1017/RDC.2020.41

Reuter, B., Hagenmuller, P., & Eckert, N. (2025). Trends in avalanche problems in the French Alps between 1958 and 2020. Cold Regions Science and Technology, 104555. https://doi.org/10.1016/j.coldregions.2025.104555

Reyss, J.-L., Schmidt, S., Legeleux, F., Bonté, P. (1995). Large, low background well-type detectors for measurements of environmental radioactivity. Nuclear Instruments and Methods in Physics Research Section A: Accelerators, Spectrometers, Detectors and Associated Equipment 357(2-3), 391–397. https://doi.org/10.1016/0168-9002(95)00021-6

Rome, S., Giorgetti, J.-P. (2007). La montagne corse et ses caractéristiques climatiques. Météorologie 59, 39-50. https://doi.org/10.4267/2042/14846

Sabatier, P., Dezileau, L., Briqueu, L., Colin, C., Siani, G. (2010). Clay minerals and geochemistry record from northwest Mediterranean coastal lagoon sequence: Implications for paleostorm reconstruction. Sedimentary Geology 228(3-4), 205–217. https://doi.org/10.1016/j.sedgeo.2010.04.012

Sabatier, P., Moernaut, J., Bertrand, S., Van Daele, M., Kremer, K., Chaumillon, E., Arnaud, F. (2022). A Review of Event Deposits in Lake Sediments. Quaternary 5, 34. https://doi.org/10.3390/quat5030034

Sabatier, P., Nicolle, M., Piot, C., Colin, C., Debret, M., Swingedouw, D., Perrette, Y., Bellingery, M.-C., Chazeau, B., Develle, A.-L., Leblanc, M., Skonieczny, C., Copard, Y., Reyss, J.-L., Malet, E., Jouffroy-Bapicot, I., Kelner, M., Poulenard, J., Didier, J., Arnaud, F., Vannière, B. (2020). Past African dust inputs in the western Mediterranean area controlled by the complex interaction between the Intertropical Convergence Zone, the North Atlantic Oscillation, and total solar irradiance. Climate of the Past 16(1), 283–298. https://doi.org/10.5194/cp-16-283-2020

Schläppy, R., Jomelli, V., Grancher, D., Stoffel, M., Corona, C., Brunstein, D., Eckert, N., Deschatres, M. (2013). A New Tree-Ring-Based, Semi-Quantitative Approach for the Determination of Snow Avalanche Events: use of Classification Trees for Validation. Arctic, Antarctic, and Alpine Research 45(3), 383–395. https://doi.org/10.1657/1938-4246-45.3.383

Schweizer, J., Bruce Jamieson, J., & Schneebeli, M. (2003). Snow avalanche formation. Reviews of Geophysics, 41(4). https://doi.org/10.1029/2002RG000123

Seierstad, J., Nesje, A., Dahl, S.O., Simonsen, J.R. (2002). Holocene glacier fluctuations of Grovabreen and Holocene snow-avalanche activity reconstructed from lake sediments in Grningstlsvatnet, western Norway. The Holocene 12(2), 211–222. https://doi.org/10.1191/0959683602hl536rp

Sletten, K., Blikra, L. H., Ballantyne, C. K., Nesje, A., and Dahl, S. O. 2003. Holocene debris flows recognized in a lacustrine sedimentary succession: sedimentology, chronostratigraphy and cause of triggering. The Holocene, 13(6), 907–920, https://doi.org/10.1191/0959683603hl673rp

Stoffel, M., Bollschweiler, M., Hassler, G. (2006). Differentiating past events on a cone influenced by debris-flow and snow avalanche activity – a dendrogeomorphological approach. Earth Surface Processes and Landforms: The Journal of the British Geomorphological Rsearch Group 31(11), 1424–1437. https://doi.org/10.1002/esp.1363

Techel, F., Jarry, F., Kronthaler, G., Mitterer, S., Nairz, P., Pavšek, M., Valt, M., & Darms, G. (2016). Avalanche fatalities in the European Alps: long-term trends and statistics. Geographica Helvetica, 71(2), 147-159. https://doi.org/10.5194/gh-71-147-2016

Thys, S., Van Daele, M., Praet, N., Jensen, B., Van Dyck, T., Haeussler, P., Vandekerkhove, E., Cnudde, V., De Batist, M. (2019). Dropstones in Lacustrine Sediments as a Record of Snow Avalanches—A Validation of the Proxy by Combining Satellite Imagery and Varve Chronology at Kenai Lake (South-Central Alaska). Quaternary 2(1), 11. https://doi.org/10.3390/quat2010011

Valéry, A., Andréassian, V., Perrin, C. (2014). 'As simple as possible but not simpler': What is useful in a temperature-based snow-accounting routine? Part 2 – Sensitivity analysis of the Cemaneige snow accounting routine on 380 catchments. Journal of Hydrology 517, 1176–1187. https://doi.org/10.1016/j.jhydrol.2014.04.058

Vasskog, K., Nesje, A., Støren, E.N., Waldmann, N., Chapron, E., Ariztegui, D. (2011). A Holocene record of snow-avalanche and flood activity reconstructed from a lacustrine sedimentary sequence in Oldevatnet, western Norway. The Holocene 21(4), 597–614. https://doi.org/10.1177/0959683610391316

Verfaillie, D., Lafaysse, M., Déqué, M., Eckert, N., Lejeune, Y., & Morin, S. (2018). Multi-component ensembles of future meteorological and natural snow conditions for 1500 m altitude in the Chartreuse mountain range, Northern French Alps. The Cryosphere, 12(4), 1249-1271. https://doi.org/10.5194/tc-12-1249-2018

Vidal, J., Martin, E., Franchistéguy, L., Baillon, M., Soubeyroux, J. (2010). A 50-year high-resolution atmospheric reanalysis over France with the Safran system. International Journal of Climatology 30(11), 1627–1644. https://doi.org/10.1002/joc.2003

Weltje, G.J., Bloemsma, M.R., Tjallingii, R., Heslop, D., Röhl, U., Croudace, I.W. (2015). Prediction of Geochemical Composition from XRF Core Scanner Data: A New Multivariate Approach Including Automatic Selection of Calibration Samples and Quantification of Uncertainties. In Croudace, I.W., Rothwell, R.G. (Eds.), Micro-XRF Studies of Sediment Cores, Developments in Paleoenvironmental Research. Springer Netherlands, Dordrecht, pp. 507–534. https://doi.org/10.1007/978-94-017-9849-5_21

Wilhelm, B., Nomade, J., Crouzet, C., Litty, C., Sabatier, P., Belle, S., Rolland, Y., Revel, M., Courboulex, F., Arnaud, F., Anselmetti, F.S. (2016). Quantified sensitivity of small lake sediments to record historic earthquakes: Implications for paleoseismology. Journal of Geophysical Research: Earth Surface 121(1), 2–16. https://doi.org/10.1002/2015JF003644

How to cite: Sabatier, P., Brigode, P., Bisquert, A., Eckert, N., Giacona, F., Deschâtres, M., Bauve, V., Kelner, M., Debret, M., Bellingery, M.-C., Copard, Y., Malet, E., Didier, J., Huneau, F., Garel, E., & Vannière, B. (2025). Wet snow avalanches on Corsica Island: a long-term perspective from lake sediments. Sedimentologika, 3(1), 1-21. https://doi.org/10.57035/journals/sdk.2025.e31.1669